Gamma-hydroxybutyrate increases brain resting-state functional connectivity of the salience network and dorsal nexus in humans

Bosch, Oliver G ; Esposito, Fabrizio ; Dornbierer, Dario ; Havranek, Michael M ; von Rotz, Robin ; Kometer, Michael ; Staempfli, Philipp ; Quednow, Boris B ; Seifritz, Erich

Abstract: According to the triple network hypothesis the brain is equipped with three core neurocognitive networks: the default mode (DMN), the salience (SN), and the central executive (CEN) network. Moreover, the so called dorsal nexus, has met growing interest as it is a hub region connecting these three networks. Assessment of resting-state functional connectivity (rsFC) of these networks enables the elucidation of drug-induced brain alterations. Gamma-hydroxybutyrate (GHB) is a GHB/GABA-B receptor agonist that induces a paradoxical state of mixed stimulation and sedation at moderate doses, which makes it a valuable tool to investigate neural signatures of subjective drug effects. Employing a placebo-controlled, double-blind, randomized, cross-over design, we assessed the effects of GHB (35 mg/kg p. o.) in 19 healthy male subjects on DMN-, SN-, CEN-, and dorsal nexus-rsFC measured by functional magnet resonance imaging and applying independent component as well as seed-based analyses, while subjective drug effects were investigated using visual analog scales (VAS). Subjectively, GHB increased VAS ratings of a general drug effect, stimulation, and sedation. Intrinsic DMN-, and CEN-rsFC remained largely unchanged under GHB, but the drug increased SN-DMN-rsFC and SN-dorsal nexus-rsFC, while dorsal nexus-rsFC was reciprocally increased to both the SN (right anterior insula) and to the CEN (right middle frontal gyrus). Increased sedation significantly predicted the observed SN-dorsal nexus-rsFC. In conclusion, GHB generates a unique stimulant/sedative subjective state that is paralleled by a complex pattern of increased functional connectivity encompassing all three core neurocognitive networks of the brain, while increased SN-dorsal nexus-rsFC was demonstrated to be a potential signature of the sedative component of the drug effect.

DOI: https://doi.org/10.1016/j.neuroimage.2018.03.011

increases brain resting-state functional connectivity of the salience network and dorsal nexus in humans. NeuroImage, 173:448-459.
DOI: https://doi.org/10.1016/j.neuroimage.2018.03.011

Gamma-hydroxybutyrate increases brain resting-state functional connectivity of the salience network and dorsal nexus in humans

Oliver G. Bosch[a,b,*], MD, Fabrizio Esposito[c], PhD, Dario Dornbierer[a,b], Msc, Michael M. Havranek[a], MD, PhD, Robin von Rotz[a,b], BSc, Michael Kometer[a], PhD, Philipp Staempfli[d], PhD , Boris B. Quednow[b,e], PhD, Erich Seifritz[a,e], MD

[a]*Department of Psychiatry, Psychotherapy and Psychosomatics, Psychiatric Hospital of the University of Zurich, Switzerland*
[b]*Experimental and Clinical Pharmacopsychology, Department of Psychiatry, Psychotherapy and Psychosomatics, Psychiatric Hospital of the University of Zurich, Switzerland*
[c]*Department of Medicine, Surgery and Dentistry "Scuola Medica Salernitana", University of Salerno, 84081 Baronissi, Italy*
[d]*MR-Center of the Department of Psychiatry, Psychotherapy and Psychosomatics and the Department of Child and Adolescent Psychiatry, Psychiatric Hospital of the University of Zurich, 8032 Zurich, Switzerland*
[e]*Neuroscience Center Zurich, University and ETH Zurich, Switzerland*

Archival Report to be submitted to: *NeuroImage*

Version: February 20th, 2018

Manuscript Characteristics:
Number of words in the abstract: 260
Number of words in the article: 7463
Number of references: 86
Number of figures: 7
Number of tables: 0
Supplementary material: yes

***Corresponding author:**
Oliver G. Bosch, MD
Department of Psychiatry, Psychotherapy and Psychosomatics
Psychiatric Hospital, University of Zurich
Lenggstrasse 31, CH-8032 Zurich, Switzerland
Phone: +41-44-384-2357
Fax : +41-44-383-4456
E-Mail: oliver.bosch@bli.uzh.ch

ABSTRACT

According to the triple network hypothesis the brain is equipped with three core neurocognitive networks: the default mode (DMN), the salience (SN), and the central executive (CEN) network. Moreover, the so called dorsal nexus, has met growing interest as it is a hub region connecting these three networks. Assessment of resting-state functional connectivity (rsFC) of these networks enables the elucidation of drug-induced brain alterations. Gamma-hydroxybutyrate (GHB) is a GHB/GABA-B receptor agonist that induces a paradoxical state of mixed stimulation and sedation at moderate doses, which makes it a valuable tool to investigate neural signatures of subjective drug effects. Employing a placebo-controlled, double-blind, randomized, cross-over design, we assessed the effects of GHB (35 mg/kg p.o.) in 19 healthy male subjects on DMN-, SN-, CEN-, and dorsal nexus-rsFC measured by functional magnet resonance imaging and applying independent component as well as seed-based analyses, while subjective drug effects were investigated using visual analog scales (VAS). Subjectively, GHB increased VAS ratings of a general drug effect, stimulation, and sedation. Intrinsic DMN-, and CEN-rsFC remained largely unchanged under GHB, but the drug increased SN-DMN-rsFC and SN-dorsal nexus-rsFC, while dorsal nexus-rsFC was reciprocally increased to both the SN (right anterior insula) and to the CEN (right middle frontal gyrus [MFG]). Increased sedation significantly predicted the observed SN-dorsal nexus-rsFC. In conclusion, GHB generates a unique stimulant/sedative subjective state that is paralleled by a complex pattern of increased functional connectivity encompassing all three core neurocognitive networks of the brain, while increased SN-dorsal nexus-rsFC was demonstrated to be a potential signature of the sedative component of the drug effect.

Key words

Fronto-parietal network, attention network, intrinsic connectivity, pharmaco-fMRI, sodium oxybate, dorsomedial prefrontal cortex

Abbreviations

ACC: anterior cingulate cortex; ANOVA: analysis of variance; ASL: arterial spin labeling; CEN: central executive network; CSF: cerebro-spinal fluid; dlPFC: dorsolateral prefrontal cortex; DMN: default mode network; dmPFC: dorsomedial prefrontal cortex; FD: frame wise displacement; GHB: gamma-hydroxybutyrate; ICA: independent component analysis; MFG: middle frontal gyrus; Nacc: nucleus accumbens; PCC: posterior cingulate cortex; ROI: region of interest; rsFC: resting-state functional connectivity; RSN: resting-state network; SN: salience network; sogICA: self-organizing group-level ICA; VAS: visual analog scales; VN: visual network; VTA: ventral tegmental area; WM: white matter.

1. INTRODUCTION

The understanding of the relationship between brain activity and subjective experience, including their coordinated manipulation by pharmacological interventions, is fundamental for the identification of brain function and the development of innovative treatment of psychiatric conditions. A valid method to investigate such drug-induced functional brain alterations is pharmaco-functional magnetic resonance imaging (fMRI) measuring blood oxygenation level-dependent (BOLD) signals. Specifically, resting-state functional connectivity (rsFC) can reveal brain signatures of pharmacological compounds and relationships between brain network activity patterns and subjective phenomena (Salmeron and Stein, 2002). The so-called triple network model unifies the three core neurocognitive large-scale brain networks, the default mode network (DMN), the salience network (SN), and the central executive network (CEN), providing a better understanding of brain function and dysfunction (Menon, 2011). The DMN shows the strongest BOLD activity during rest (Buckner et al., 2008), comprises cortical midline structures such as the precuneus and medial frontal cortex as well as the inferior parietal lobule (Fox and Raichle, 2007, Raichle et al., 2001), and is involved in the recollection of prior experiences, emotional processing, and other self-referential mental activities (Raichle, 2015). The posterior cingulate cortex (PCC) is commonly considered as the central node of the DMN (Khalsa et al., 2014). The SN is active both during rest and during task-related activity and is understood as network with a switching function between the DMN and the CEN, identifying biologically and cognitively relevant stimuli to guide adaptive behavior (Menon, 2015). It is anchored in the anterior insula and the dorsal part of the anterior cingulate cortex (ACC), but also includes subcortical structures such as the amygdala, the ventral striatum/ nucleus accumbens Nacc (Nacc), and the ventral tegmental area (VTA) (Craig, 2009, Gogolla et al., 2014, Menon and Uddin, 2010). Finally, the CEN is anchored in the dorsolateral prefrontal cortex and lateral posterior parietal cortex and is mainly active during task-related cognitive control activity involving working memory, problem solving, and decision making or other goal-directed behavior

(Koechlin and Summerfield, 2007, Niendam et al., 2012, Seeley et al., 2007). The CEN in the here used definition overlaps or is part of previously described networks such as the fronto-parietal network (Smith et al., 2009, Spreng et al., 2013, van den Heuvel et al., 2009), referring to its anatomical location, and attention network (Markett et al., 2014, Toro et al., 2008), focusing on a functional aspect. Intriguingly, a connectivity hub in the dorsomedial prefrontal cortex (dmPFC), the so-called dorsal nexus, was discovered to serve as an interface between the DMN, SN, and CEN in depressed patients (Sheline et al., 2010). It was postulated that dorsal nexus-rsFC alterations may serve as biomarkers for antidepressant effects, which was supported by studies using antidepressant interventions including citalopram (McCabe et al., 2011), ketamine (Scheidegger et al., 2012), and sleep deprivation (Bosch et al., 2013).

Gamma-hydroxybutyrate (GHB), a mixed GABA-B (Engberg and Nissbrandt, 1993) and GHB receptor (Benavides et al., 1982) agonist, is an interesting neuropsychopharmacological research tool as it exerts a paradoxical state of mixed stimulation and sedation, among other more specific drug effects. In humans, GHB strongly influences behaviors related to core human autonomic functions such as control of food intake, sexual behavior, and sleep-wake regulation (Bosch and Seifritz, 2016). Moreover, the drug was shown to exert prosocial (Bosch et al., 2015, Sumnall et al., 2008) and prosexual effects (Kapitany-Foveny et al., 2015), latter of which are associated with increased activity in the ACC and Nacc (Bosch et al., 2017b). Moreover, GHB increases regional cerebral blood flow (rCBF) in the right anterior insula and bilateral ACC, which was correlated with increased body and emotion awareness (Bosch et al., 2017a). On a subjective level, GHB induces a mixed stimulant-sedative pattern, including stimulation, sedation, euphoria, disinhibition, and enhanced vitality (Bosch et al., 2015). Thus, GHB shares properties usually attributed to both sedatives such as benzodiazepines, z-drugs, or alcohol, as well as stimulants such as methylphenidate, amphetamines, or cocaine (Bosch and Seifritz, 2016). This specific pharmacological profile is clinically utilized in neuropsychiatric disorders such as narcolepsy, alcohol withdrawal, fibromyalgia, and binge-eating syndrome. Additionally,

the subjective, prosocial and prosexual effects are instrumentalized by non-medical users (Teltzrow and Bosch, 2012). Taken together, these properties led to the suggestion that GHB might be an interesting experimental antidepressant agent (Bosch et al., 2012, Mamelak, 2009).

Functional brain signatures of sedative and stimulant drugs have been described using rsFC, but the effects of GHB are unknown yet. As GHB primarily acts agonistically on GABA neurotransmission and has strong secondary effects on the dopamine system (Bosch and Seifritz, 2016), it is conceivable that GHB produces rsFC alterations as seen after GABA- and/or dopaminergic drug administration. Sedative GABAergic drugs such as zolpidem (Licata et al., 2013), midazolam (Greicius et al., 2008, Kiviniemi et al., 2005, Liang et al., 2015), and alcohol (Esposito et al., 2010, Khalili-Mahani et al., 2012) were consistently found to increase rsFC with and within the SN and/or CEN, while simultaneously reducing intrinsic DMN-rsFC. By contrast, the findings on the effect of stimulants on rsFC appear to be more inconsistent. RsFC reductions were found for cocaine within the primary visual and motor cortices (Li et al., 2000), for dexamphetamine within DMN, SN, and CEN (Schrantee et al., 2016), for methylphenidate in the thalamus, the supplementary motor area (Konova et al., 2015), and the mesolimbic reward system (Ramaekers et al., 2013). On the other hand, mixed patterns of rsFC increase and reduction were found for methylphenidate encompassing motor and limbic (Farr et al., 2014, Kline et al., 2016, Mueller et al., 2014), as well as DMN, SN, and CEN nodes (Sripada et al., 2013). Moreover, the stimulant modafinil, which is like GHB clinically used for narcolepsy treatment, increased rsFC between the insula and the putamen, the superior frontal gyrus, and the ACC (Cera et al., 2014), and of the left CEN to the pre-supplementary motor area (preSMA), the occipital pole, and the inferior parietal gyrus (Esposito et al., 2013) in healthy subjects. Unfortunately, no information was given regarding putative correlations between subjective and neural data in any of these previous studies.

To identify GHB-specific functional brain alterations and their possible relationships to putative subjective drug-effects, we assessed rsFC at baseline and + 34 min, + 59 min, and + 79 min post challenge with 35 mg/kg p.o. vs. placebo in healthy male subjects. Visual analog scales (VAS) were used to measure subjective feelings of the general drug effect, stimulation, and sedation. We hypothesized that GHB increases subjective sedation and stimulation, which correlates with rsFC alterations of the DMN, SN, CEN, and the dorsal nexus.

2. MATERIAL AND METHODS

2.1 Design and Study Subjects

A randomized, double-blind, placebo-controlled, balanced, crossed within-subject design was used. All subjects were non-smoking, healthy males. Nineteen subjects with a mean age of 23.5 years (standard deviation: ±3.6*, range:* 20-36), a mean verbal intelligence quotient (IQ) of 113.4 (±18.4, 88-145), and a mean weight of 72.2 kg (±7.4, 59-85) participated. Subjects were recruited by online advertisings and underwent a medical and psychiatric examination applying the Structured Clinical Interview for DSM-IV Axis-I Disorders (First et al., 2002). Exclusion criteria were any DSM-IV psychiatric disorder, neurological disorder, severe medical disease, left-handedness, and regular illegal drug use (lifetime use >5 occasions, with exception of occasional cannabis use), latter assessed by using the Interview for Psychotropic Drug Consumption (Quednow et al., 2004). Subjects performed a German vocabulary test, the Mehrfachwahl-Wortschatz-Intelligenztest (Lehrl, 2005), to estimate the verbal IQ. They had to abstain from drinking alcohol 24 h before the experimental sessions and from drinking caffeinated beverages during the course of the study days. Abstinence from illegal drugs at the test sessions was ensured by semi-quantitative drug urine tests (Dimension RXL Max, Siemens, Erlangen, Germany). The study was approved by the Cantonal Ethics Committee of Zurich and by Swissmedic and registered at ClinicalTrials.gov (NCT02342366). All subjects gave written informed consent and were financially compensated.

2.2 Procedure

GHB and placebo were applied in two order-balanced sessions separated by seven days. On both test days, subjects completed an fMRI paradigm (Bosch et al., 2017b) on a Philips Achieva 3T whole-body MR-unit equipped with a 32-channel head coil (Philips Medical Systems, Best, The Netherlands). The experiment started with a T1-weighted anatomical brain scan, a baseline rsFC (, all 6 min duration), and an arterial spin labeling (ASL, all 5 min duration) scan.

Subsequently, subjects were taken out of the scanner and were orally administered with a single dose of GHB (35 mg/kg) or placebo (t=0 min) (order-balanced). As C_{max} of GHB can be expected after about 40 min (Liechti et al., 2016), the fMRI challenge session began at t +30 min followed by a challenge rsFC (+34 min) and an ASL (+40 min) scan. Thereafter, subjects underwent the first run of the fMRI paradigm (a visual stimulation task, t=+48 min). After that, another rsFC (+59 min) and subsequent ASL (+65 min) scan was performed which was followed by the second run of the fMRI paradigm (t=+ 70 min). At the end of the experiment, final rsFC (+79 min) and ASL (t=+ 85 min) scans were acquired again after which subjects were taken out of the scanner and debriefed. Subjective drug effects were measured using computerized VAS (100mm scale, with item name and according statement, e.g. 'I feel a drug effect' for *general drug effect*, with 'not at all' and 'strongly' on the poles of the scale, selection via hand tool with scroll function) assessing *general drug effect, sedation, relaxation, stimulation, euphoria, body awareness, emotion awareness, sexual arousal, dizziness*, and *nausea* at time points t=-25 min before and +45 min, +55 min, +68 min, +77 min, and +93 min after drug/placebo administration in the scanner but not during scans (see **supplementary figures 1 and 2**) (Abanades et al., 2006, Bosch et al., 2015, Thai et al., 2007). Experimental sessions lasted 200 min. Here, the GHB effects on VAS items general drug effect, sedation, and stimulation and rsFC data are presented, while the ASL and task-related fMRI data were published elsewhere (Bosch et al., 2017a, Bosch et al., 2017b).

2.3 MRI Data Acquisition

rsFC time series were acquired with a sensitivity-encoded single-shot echo-planar imaging sequence (SENSE-sshEPI) (45). The rsFC protocol used the following acquisition parameters: TE=35ms, TR=2000ms, flip angle=82°, FOV=22cm2, acquisition matrix=80x80 (in plane voxel size=2.75x2.75mm2), 32 contiguous axial slices (placed along the anterior-posterior commissure plane) with a slice thickness of 4mm, and a SENSE factor R=2.0. For structural reference, a

magnetization prepared rapid gradient-echo (MP-RAGE) T1-weighted anatomical scan was acquired with the following parameters: TR/TE=9.3/4.6ms, flip angle=8°, 160 sagittal slices, FOV 240×240 mm, voxel size=1×1×1mm.

2.4 MRI Data Preprocessing

Standard image data preparation and pre-processing, as well as statistical analysis and visualization were performed with the software BrainVoyager QX (Brain Innovation BV, The Netherlands). Functional data preprocessing included a correction for slice scan timing acquisition, a 3D rigid body motion correction, a spatial smoothing (gaussian kernel of 6 mm full-width-half-maximum), a temporal high-pass filter with cut-off set to 0.0080 Hz per time-course and a temporal low-pass filter (gaussian kernel of 3 s). After 3D rigid body correction, a 24-parameter model of head motion was created for each data set with the purpose of regressing out any residual effects of motion from each data set prior to functional connectivity estimation. This model incorporates the 6 head motion translation and rotation parameters estimated during 3D rigid body correction, the 6 first order derivatives of the motion parameters, and the 12 corresponding squared items (Friston et al., 1996, Satterthwaite et al., 2013).
Structural and functional data were co-registered and spatially normalized to the Talairach standard space using a twelve parameter affine transformation. In the course of this procedure, the functional images were resampled to an isometric 3x3x3 mm^3 grid covering the entire Talairach box. Nuisance physiological signals from white matter (WM) and cerebro-spinal fluid (CSF) were estimated from each data set by segmenting the WM and the ventricles in the normalized T1 volumes and calculating the average WM and CSF signals from these volumes. Following previous recommendations (Geerligs et al., 2017, Shirer et al., 2015, Varikuti et al., 2017), all 24 motion parameters, together with the WM and CSF signals, were regressed out from each time-course at each voxel.

2.5 Statistical Analysis of VAS Data

For the analyses of VAS scales, repeated measures analysis of variance (ANOVA) with drug (2-fold: GHB, placebo) and time (6-fold) as within-subject factors and session (GHB-first vs. placebo-first) as between-subject factor were applied using SPSS®22.0 for Windows. Bonferroni-corrected paired t-tests were applied for post hoc treatment comparisons (placebo vs. GHB). All confirmatory statistical comparisons were carried out at a significance level of $p<.05$ (two-tailed).

2.6 Statistical Analysis of MR Images

2.6.1. Independent Component Analysis of Resting-state fMRI Networks

A hierarchical independent component analysis (ICA) approach was performed to study the functional connectivity of resting-state networks (RSNs) under changing experimental conditions similar to previous studies (see, e. g., (Esposito et al., 2014)). First-level (single-subject, single-scan) and second-level (group) ICA analyses were performed on the pre-processed functional time series using two plug-in extensions of BrainVoyager QX, respectively implementing the so-called fastICA algorithm (Hyvarinen, 1999) and the self-organizing group-level ICA (sogICA) algorithm (Esposito et al., 2005).

For each subject and each scan, 30 independent components were extracted using fastICA, roughly corresponding to 1/6 of the number of time points (see, e. g. (Greicius et al., 2007, Shirer et al., 2015). Minimum description length (MDL) (Rissanen, 1978), as implemented in FSL MELODIC command line program (https://fsl.fmrib.ox.ac.uk/fsl/fslwiki/MELODIC), was also used to analytically justify the number of components extracted from each data set.

All 30 ICA component maps from the baseline scans of the first experimental session (n=18) were “clustered” at the group level using the sogICA algorithm (Esposito et al., 2005), yielding 30

group ICA component t-statistic maps as follows. The 30 clusters of 18 components (one per subject) were entered into a 1-factor random-effect ANOVA with 1 within-subject factor (*cluster membership*) with 30 levels (one per component) and subjects as random observations. From this 1-way ANOVA, we produced 1-sample t-test maps (one for each cluster) and extracted the components lay-out (mask) by applying a voxel-level threshold of p=0.05 (Bonferroni corrected for multiple voxel-level comparisons). To identify (and label) an interested network, the component mask was preliminary applied to ten external *well-matched* ICA components available on line (http://www.fmrib.ox.ac.uk/datasets/brainmap+rsns/) (Smith et al., 2009). The best matching between a group ICA component map and an RSN component map resulted from the highest average ICA score inside the mask. The selected (and matched) group ICA component masks were thus used to create (treatment-independent) internal templates for DMN, SN, left and right CEN, and VN, and used to select the individual ICA components from each individual scan (baseline, challenge [+ 34 min], + 59 min, + 79 min). Each internal RSN template mask was used to select one best-fitting RSN component per subject and per scan for the second-level random-effects statistical analysis (see 2.6.3). The best-fitting RSN component was the component reporting the highest goodness-of-fit score, defined as the difference between the average component score inside the mask minus the average component score outside the mask (Esposito and Goebel, 2011, Greicius et al., 2004).

For each RSN of interest, all selected ICA component maps were entered into the second-level (group-level) statistical analysis (see paragraph 2.6.3). Importantly, these were all *native* ICA components, i.e. ICA maps (and time-courses) directly estimated from the fastICA algorithm applied to each data set, and were not the result of a matrix back-projection or dual (spatio-temporal) regression from groups of ICA components back to individual data sets. The difference between the two types of group-level ICA approaches (individual vs. aggregate) has been previously reviewed and discussed by (Esposito and Goebel, 2011).

Besides the within-network connectivity changes within a given RSN of interest (see 2.6.3), the between-network connectivity changes (between two RSNs) were also assessed from the ICA component time-courses. Thus, the scan- and subject-specific ICA component time-courses were extracted for all individual ICA components selected as SN, DMN, R- and L-CEN and correlation coefficients (Pearson's r) were computed per scan per subject for all possible pairs of ICA component time-courses for each individual scan. The resulting connectivity matrix was used for a second-level (group-level) statistical analysis after Fisher transformation from r to z values. Thereby, paired t-tests were conducted to compare correlation z values between the SN and DMN, the SN, the CENs and between the DMN and the CENs across different experimental conditions (GHB vs. placebo at challenge [+ 34 min] and challenge vs. baseline for GHB and placebo sessions). Mean connectivity regression of the within-subject connectivity matrices (Geerligs et al., 2017, Yan et al., 2013) was also performed, albeit without pre-whitening due to the choice of low-pass filtering the original time-courses. Bonferroni correction was applied to the p-values to correct for the multiple tests (over all inter-network connectivities and all experimental conditions).

2.6.2 Seed-based Functional Connectivity Analysis

A seed-based analysis was performed to study the functional connectivity from the PCC and dorsal nexus to the entire brain identically to previous studies (Bosch et al., 2013, Scheidegger et al., 2012). These seeds were selected as the PCC is commonly considered as the central node of the DMN (Khalsa et al., 2014), while the dorsal nexus seed was discovered to be a candidate biomarker for an antidepressant treatment response (Sheline et al., 2010), which was further investigated in previous studies of ours (Bosch et al., 2013, Scheidegger et al., 2012). To compute functional connectivity maps corresponding to a selected seed region of interest (ROI), the mean regional time-course was extracted from all ROI voxels and correlated against all voxels of the brain. The (rationale for) definition of these two ROIs was identical to the previous

works (see (Bosch et al., 2013, Scheidegger et al., 2012) for all details). Separate correlation maps were produced for each subject, condition, and ROI. The correlation maps were applied the Fisher's r-to-z transform z=0.5 Ln [(1+r)/(1−r)] before entering the second-level random-effects statistical analysis (see paragraph 2.6.3).

Because seed-based connectivity estimates can be affected by micro-movements (Power et al., 2012), a supplementary motion analysis was performed to control for possible effects of residual motion artifacts in the data. Following Power et al. (2012), the frame wise displacement (FD) was calculated for each time point of each scan using the motion estimates obtained at the preprocessing stage. Then, prior to nuisance regression, volume censoring was applied to all volumes exhibiting an FD above 0.2 mm as well as to the two volumes preceding and following such volumes in the time-series (Power et al., 2015). For the second-level (group-level) analyses, the mean FD was considered as a covariate of no interest and regressed out from the series of z-values (across subjects) to remove any further residual effects of motion from the second-level analysis.

2.6.3 Group-level Analysis of Functional Connectivity Maps

For the whole-brain voxel-based rsFC analysis, all Talairach-normalized functional connectivity z-maps (either ICA z-maps for each network of interest or seed-based correlation z-maps) from all 144 rsFC data sets (18 subjects, 2 session, 4 repeated scans) were combined and entered into the analysis of covariance module of BrainVoyager QX. Here, a 3-way (4x2x2) mixed-effects ANOVA design was specified with two within-subject factors (*scan*, *treatment*), and one between-subject factor (*session*). Following the experimental design, the factor *scan* was assigned with four levels (baseline, t=+34 min, t=+59 min, t=+79 min), the factor *treatment* with two levels (GHB, placebo) and the factor *session* with two levels (GHB-first, placebo-first). All interactions between and among all three factors were also added to the model. The *session*

factor was a between-subject factor because half of the subjects had the GHB session as first session (and the placebo session as second session) and half of the subjects had the GHB session as second session (and the placebo session as second session). This introduced a potential session effect (GHB-first vs. placebo-first) that was accounted for as a between-subject factor.

After least square model fitting, to detect any effects of systematic functional connectivity changes in relation to time, treatment and session, the t statistics for the contrast [GHB (challenge [+ 34 min]) - GHB (baseline)] vs. [placebo (challenge) - placebo (baseline)] was computed at each voxel, yielding a whole-brain t-statistic map, which was thresholded and overlaid in pseudo-color onto the average normalized T1 image. As the dynamic analysis of rsFC data across sessions and time points is intrinsically multi-factorial, a full factorial data model (3-way ANOVA) was used to produced *data-cells* in such a way to separate (and account for) the variance associated with all three possible factors (*session*, *treatment*, *scan*) and their interactions and to minimize the error variance in the contrast. However, all main and interaction effects from the full model were considered not of interest. In fact, the *session* factor captures any changes between first and second sessions regardless of these being GHB or placebo sessions, the *treatment* factor captures any changes between GHB and placebo sessions including those occurring at baseline time points and the *scan* factor captures any change between time points regardless of these occurring in GHB or placebo sessions. Moreover, any interaction among these factors would require the calculation of additional post hoc contrasts to facilitate the interpretation of any detected effects. Therefore, to reduce the burden of multiple comparisons and simplify the interpretation of the effects of interest (GHB-related changes from baseline to challenge [+ 34 min] vs. placebo-related changes from baseline to challenge) we only considered the cells *GHB-baseline*, *GHB-challenge*, *placebo-baseline* and *placebo-challenge* to calculate the main contrast of interest, albeit properly accounting for all confounding

effects in the statistics and anyway reporting the full time-course of the rsFC responses for any region exhibiting statistically significant effects.

To protect against false positives and correct for multiple comparisons, only statistically significant regional effects were displayed for compact clusters surviving the joint application of a voxel- and a cluster-level threshold, which were chosen using a non-parametric randomization approach based on Monte Carlo simulations. Namely, an arbitrary (uncorrected) threshold ($p<0.005$) was initially applied to all voxels; then, a minimum cluster size was set in such a way that an average of 5% false positive clusters were counted in 10000 randomly generated images to which the same thresholds were applied. However, due to possible concerns on the multiple comparisons problem as addressed with cluster-level correction (Eklund et al., 2016), a stricter uncorrected threshold of $p<0.001$ has been applied. To match the level of "smoothness" between the calculated and the simulated images, the resulting images were spatially filtered with the same gaussian kernel applied to the original rsFC images. For Monte Carlo simulations, a BrainVoyager QX plugin was used, implementing a 3D extension of the procedure described in (Forman et al., 1995) for multiple comparison correction. In the course of this procedure, the smoothness for the images was estimated as the full-width-at-half-maximum of the gaussian kernel using the 3D extension of the formula in (Forman et al., 1995).

2.6.4 Region-of-interest based Analysis of Functional Connectivity Maps

For regions identified in the above analysis, mean regional functional connectivity z-values were extracted for each scan, session and subject, and used for ROI based correlation analyses with subjective VAS measures *of sedation* and *stimulation*. One subject was excluded from these analyses due to missing VAS values in one of the sessions.

Correlation analyses entailed with calculating the regional functional connectivity z value and VAS changes (∆_Z and ∆_VAS) between challenge (t=+34 min) and baseline (t=-20 min) time points, and then linearly regressing ∆_Z values vs. ∆_VAS in each separate treatment (GHB or placebo). Given the small sample (and the noisy ∆_Z measures), to make the correlation findings less susceptible to outliers in the data, we used a robust (weighted) linear regression model and anyway reported a box plot of ∆_Z measures (with medians, quartiles and outliers) next to each scatter plot (with trend lines). Moreover, in order to dissociate between mechanisms of sedation and stimulation, a robust (weighted) multivariate regression analysis was performed in Matlab® (The Mathworks, Inc., Natick, MA, United States, www.mathworks.com) with the function *robustfit* and default settings (iteratively reweighted least squares with a bisquare weighting function), where the changes in VAS scores of sedation (∆_VAS *sedation*) and stimulation (∆_VAS *stimulation*) were included as two independent predictors for the FC changes (∆_Z FC), and the statistical significance of each linear trend is reported (for baseline and challenge [+ 34 min] time points).

3. RESULTS

3.1 Subjective Ratings

In drug × time (2×6) ANOVAs with session as between-subject factor, the general drug effect, sedation, and stimulation VAS ratings showed significant time ($F(5,25)=11.1–17.7$, $p<.001$), drug ($F(1,29)=19.2–29.7$, $p<.001$) and drug × time interactions ($F(5,25)=5.1–10.4$, $p<.01$-$.001$). The factor session (GHB-first vs. placebo-first) was not significant ($F(1,29)=0.00–0.06$, $p=.81–.95$). Paired t-test (Bonferroni-corrected) revealed significant GHB effects for all three VAS measures in most of the time points after drug administration (**Figure 1**).

- Figure 1 -

3.2 Neuroimaging

3.2.1 Motion and Dimensionality Analysis of rsFC time-series

Prior to nuisance and motion regression, the mean FD was estimated from each time-series and statistically assessed across experimental conditions (time points and sessions). For each condition, the mean FD was far below the critical threshold of 0.5 mm indicated by Power et al. (2012) for data set exclusion (see **supplementary figure 3**). However, it was significantly higher at challenge (t=+34 min), post-task 1 (t=+59 min) and post-task 2 (t=+79 min) time points compared to baseline (t=-20 min) (1 sample paired t-test, $p<0.05$), and was also slightly higher in GHB, compared to placebo, sessions, albeit only at post-task 1 (t=+59 min) (1 sample paired t-test, $p=0.03$), a time point which was not selected for the main contrast of interest in second-level analyses. Although the mean FD was not significantly different between GHB and placebo sessions at baseline (t=-20 min) and challenge (t=+34 min) time points, this measure was considered as covariate of no interest for the second-level analysis and was regressed out from the series of functional connectivity z-maps (as resulting from either ICA or seed-based analyses) entering the ANOVA data model (and the contrast calculation).

After nuisance and motion regression, MDL was used to analytically estimate the number of ICA components in each data set. In average, MDL yielded 31±4 (mean ± SD) components per data set which analytically justifies the empirical choice of extracting 30 components per scan (see also, e. g. (Shirer et al., 2015).

3.2.2 ICA-based Analysis of Resting-state Networks

We performed the sogICA on all baseline scans and, following Menon (Menon, 2011, 2015), selected the components corresponding to the DMN, SN, CEN, and VN. As often reported in the literature, the CEN was found as two lateralized networks (right CEN and left CEN) (**Figure 2).** Starting from the maps, we created the network masks for extracting the homologue network best-fitting ICA components from each data set (i.e. from each subject, at each time point) and examined the direct GHB effects (GHB vs. placebo) between challenge (+ 34 min) and baseline time points, both within the network (via voxel-wise analysis) and between the networks (via correlation analysis). The inter-network connectivity analysis was restricted to the networks included in the Menon model as the VN served only as a control network, where no drug effects are expected.

When comparing challenge (t=+34 min) vs. baseline (t=-20 min) conditions, no GHB vs. placebo differential effects were found significant within the DMN, the CEN and the VN. Instead, when comparing challenge (t=+34 min) vs. baseline (t=-20 min) conditions, the differential effects of GHB vs. placebo were statistically significant ($p<.05$ cluster-level corrected, $p<.001$, uncorrected) in a region located in the dmPFC (**Figure 3**). Notably, the location of increased connectivity in the SN coincides with the a priori definition of dorsal nexus that we used in previous resting-state fMRI papers (Bosch et al., 2013, Scheidegger et al., 2012) and that, therefore, we also used here for the seed-based analysis (**Figure 4**). Moreover, under GHB, but not under placebo, the correlation between local increases in SN component scores (challenge vs. baseline) and local changes in cerebral blood flow (challenge vs. baseline) from

corresponding arterial spin labeling scans acquired in the same experiments from the same subjects (see (Bosch et al., 2017a) for details) in dmPFC/dorsal nexus is highly statistically significant (robust linear regression, p=0.0005) (**Supplementary figure 4**).

Using the ICA component time-courses, the functional connectivity between any two networks (among the DMN, the right and left CEN and the SN) in two time points (baseline, challenge) were also estimated (inter-network connectivity). From this analysis, a statistically significant increase of the inter-network connectivity between the SN and the DMN was found at challenge (t=+34 min) vs. baseline (t=-20 min) under GHB treatment (1 sample paired t-test: p=0.029 after Bonferroni correction for all pairs of networks and time points). This was not the case for placebo treatment (p>0.05). At challenge (t=+34 min), the inter-network connectivity between SN and DMN was also significantly higher for GHB vs. placebo sessions (1 sample paired t-test: p=0.048 after Bonferroni correction for all pairs of networks and time points). However, when mean connectivity regression was applied to each individual inter-network connectivity matrix, none of the inter-network connections remained statistically significant in the group analysis.

Finally, to show where, in the frequency domain, the original source of the observed functional connectivity increases occurs, the average spectral features of the SN component time-courses were extracted and are reported in **supplementary figure 5**. Considering the average of all smoothed magnitude FFT spectra of the SN component time-courses from all scans (grouped by condition and time point), these spectral plots show that, compared to placebo, at challenge (t=+34 min), GHB significantly increases the SN spectral power only within the frequency band 0.01Hz-0.04Hz (p<0.05), and significantly decreases the SN spectral power only at frequencies above 0.08Hz (p<0.05). At baseline, there are no significant differences in the spectral features between GHB and placebo sessions.

- Figures 2-4-

3.2.3 Seed-based Analysis of dorsal nexus connectivity

The seed-based analysis was performed using the PCC (to depict the DMN) as well as the dorsal nexus, as seeds, according to previous studies (Bosch et al., 2013, Scheidegger et al., 2012). However, compared to ICA-based analyses, the approach to control for the effects of motion on a within-subject level was even more stringent, as, besides the regression of WM and CSF nuisance signals and 24 motion parameters, volume censoring was also applied. More specifically, prior to nuisance and motion regression, volume censoring was also applied to all volumes exhibiting an FD above 0.2 mm as well as to the two volumes preceding and following such volumes in the time-series. Nonetheless, for all data sets, the number of *motion-free* volumes was significantly above 80% and there was no significant difference between GHB and placebo sessions at baseline and challenge time points.

We found no statistically significant differences in PCC-rsFC between GHB and placebo, which is in-line with the ICA results. In contrast, dorsal nexus-rsFC connectivity was increased to the right anterior insula and the right middle frontal gyrus (MFG) from baseline (t=-20 min) to challenge (t=+34 min), under GHB vs. placebo ($p<.05$ cluster-level corrected, $p<.001$ uncorrected) (**Figure 5**). Crucially, these two clusters of differential connectivity respectively fall within the SN and right CEN networks (**Figure 6**). Moreover, at a looser cluster-forming threshold of $p<.005$ uncorrected ($p<.05$ cluster-level corrected), we also found that the region in the right anterior insula which showed increased dorsal nexus connectivity after GHB challenge partly overlaps with one of the two regions with increased regional cerebral blood flow under GHB vs. placebo (**Figure 7)** (Bosch et al., 2017a).

- Figures 5-7-

3.2.4 Region-of-interest based Analysis of Functional Connectivity Maps

All three regions for which we detected significant changes from baseline to challenge (+ 34 min) after GHB vs. placebo were considered regions of interest and further investigated for possible correlations between the changes in the subjective effects (Δ_VAS = VAS1 vs. VAS2) from baseline to challenge and the corresponding changes in the functional connectivity values (Δ_FC) from baseline to challenge. Using stimulation and sedation subjective ratings as two independent predictors for the regional SN component scores in dorsal nexus, a robust multivariate regression analysis highlighted a statistically significant ($p<.05$) correlation between Δ_FC and Δ_VAS for *sedation,* at +34 min ($p=0.013$), but not for stimulation ($p>0.05$), under GHB, but not under placebo ($p>0.05$) (see **supplementary figure 6**). Similar trends were observed for the right anterior insula (GHB, sedation: $p=0.062$, stimulation: $p>0.1$; placebo: $p>0.1$) and the right middle frontal gyrus (GHB, sedation: $p=0.058$, stimulation: $p>0.1$; placebo: $p>0.1$), when considering the regions resulting from the seed-based analysis (see **supplementary figures 7** and **8**).

4. DISCUSSION

As expected, 35 mg/kg p.o. GHB elicited mixed sedative-stimulant effects in healthy males on the subjective level (Bosch et al., 2015). At the neuronal level, GHB increased the inter-network connectivity between SN and DMN, and the within-network connectivity of the SN to an area in the dmPFC, which highly overlapped with the previously studied dorsal nexus hub region. Reciprocally, the seed-based connectivity from the dorsal nexus was increased to the right anterior insula, which belongs to the SN, and to the right MFG, which belongs to the right CEN. In contrast, within-network functional connectivity of DMN and CEN networks remained unchanged, and, when using both sedation and stimulation subjective ratings, only sedation significantly predicted the increased SN connectivity to the dorsal nexus.

In general, the dynamic analysis of ICA spatial maps of rsFC time-series across sessions and time points is intrinsically multi-factorial and may thus reflect both changes in neural activity or connectivity and non-neural phenomena. In similar cases, more complex generative models (as an alternative to factorial models) might in principle enable the separate estimation of true neural connectivity effects and other effects on the hemodynamic compartment (Tsvetanov et al., 2016). In our case, however, the spectral plots clearly show that, even if the spatial layout of the SN component partly overlaps with vascular territories, the observed GHB-related increases in SN component time-course activity occur mainly within the so-called *slow-5* and *slow-4* frequency bands of rsFC activity (Zuo et al., 2010), whereas the reductions in the same activity are confined to higher frequencies (>0.08 Hz). As *slow-5* and *slow-4* rsFC oscillations are primarily originated (and detected) within the gray matter, whereas non-neural signals, such as respiratory and (aliased) cardiac signals that originate from the vascular territories, fall in the range of the so-called *slow-3* and *slow-2* frequency bands (Zuo et al., 2010), this observation clearly suggests that the here reported SN increases most likely reflect changes in true neural

signals rather (or more) than vascular signals[1]. This evidence is further corroborated by the highly significant correlation found between local SN component activity increases and rCBF increases in the dorsal nexus region, the latter being measured from fully independent data sets acquired from the same subjects in the same sessions and time points with the arterial spin labeling technique (Bosch et al., 2017a).

Notwithstanding the above considerations, the inter-network connectivity results (for which we unfortunately did not have the rCBF counterpart) should still be interpreted with caution. In fact, when mean connectivity regression of the within-subject connectivity matrices was applied to each data set prior to group statistics (according to Geerligs et al., 2017), these findings ceased to result statistically significant. Thus, on the one hand, albeit unlikely, we cannot completely exclude that such inter-network connectivity effects are related to the different vascular health of our subjects, which, in turn, might have determined a different global response of rsFC correlations after GHB (vs. placebo) at challenge (+ 34 min) vs. baseline. On the other hand, it should be also noted that when only six connections (from four networks) are considered, even a single connection substantially changing between conditions or time points may result in a substantial change in the overall mean connectivity in most individuals, causing the group effect to disappear in all connections when mean connectivity regression is applied. Indeed, the mean connectivity regression was shown by Geerligs et al. (2017) for cases with much bigger connectivity matrices, implicitly suggesting that this type of correction could be particularly appropriate and effective for *connectome-wide* analyses where, e. g., more than 100 regions are tested for possible connectivity changes.

Vigilance reduction, induced either by GABAergic sedative drugs such as zolpidem (Licata et al., 2013), midazolam (Greicius et al., 2008, Kiviniemi et al., 2005), and alcohol (Esposito et al., 2010, Khalili-Mahani et al., 2012), or by non-pharmacological interventions such as sleep

[1] It might be also worth noting that because ICA component time-courses are intrinsically normalized to unit variance/power any increase in this power within a limited frequency band is necessarily compensated by an equal reduction in a different frequency band.

deprivation (Bosch et al., 2013, De Havas et al., 2012, Samann et al., 2010) or falling asleep (Horovitz et al., 2009, Larson-Prior et al., 2009) have been consistently associated with reduced DMN within-network connectivity and increased connectivity of the DMN with the SN and the CEN. Comparably, high vigilance states, induced by stimulants (Cera et al., 2014, Esposito et al., 2013, Farr et al., 2014, Kline et al., 2016, Mueller et al., 2014, Sripada et al., 2013) or non-pharmacological interventions (Wang et al., 2016) have been also associated with increased and reduced connectivity of the DMN, pointing towards the necessity of a more detailed analysis of these phenomena. Interestingly, in our healthy subjects GHB induced sedation as well as stimulation, without altering rsFC within the DMN. On the other hand, SN-DMN-rsFC was increased under influence of the drug. While latter observation replicates earlier findings, the unchanged rsFC within DMN at first glance surprising, as GABAergic stimulation usually paralleled by vigilance reduction was consistently found to reduce intrinsic DMN-rsFC (see above). However, this discrepancy might be well explained by the finding that GHB unlike other GABAergic drugs consistently exerts a mixed sedative-stimulant pattern (Abanades et al., 2006, Bosch et al., 2015), in which the stimulant part might be induced by indirect dopaminergic enhancement via disinhibition of the VTA and NAcc (Bosch and Seifritz, 2016). As sedative drugs tend to reduce, whereas stimulants rather increase intrinsic DMN-rsFC, the co-occurrence of sedative and stimulant effects of GHB seem to counterbalance each other on the DMN level, resulting in no significant differences compared to placebo.

Regarding the SN, GHB not only increased its between-network connectivity to the DMN, but also increased its intrinsic rsFC to a region in the dmPFC that highly overlapped with our a priori selected dorsal nexus-seed, which is discussed as a biomarker for antidepressant treatment response (Bosch et al., 2013, McCabe et al., 2011, Scheidegger et al., 2012, Sheline et al., 2010). Increased rsFC within the SN was also reported under light sedation with midazolam in healthy subjects (Liang et al., 2015). In our subjects, GHB activates the SN, a network which provides the detection of biologically relevant internal and external stimuli to guide adaptive

behavior, and which is anchored in the anterior insula and the dorsal ACC as well as in subcortical structures such as the ventral striatum/Nacc and the VTA (Menon and Uddin, 2010, Menon, 2011, 2015). Interestingly, dorsal nexus-rsFC was reciprocally increased to the right anterior insula, and this region highly overlapped with the insular rCBF-increase that was previously demonstrated under GHB (Bosch et al., 2017a), both strengthening the assumption of a functional coupling of the SN and the dorsal nexus under the influence of the drug.

One key function of the SN is switching between DMN and CEN on the base of incoming sensory and limbic stimuli (Menon and Uddin, 2010, Menon, 2011, 2015). In our healthy subjects, the switching between the SN and DMN was directly (and globally) strengthened by GHB treatment, as suggested by the significantly increased inter-network connectivity between the SN and DMN after GHB (vs. placebo) challenge (+ 34 min) and vs. baseline. In other studies, SN-DMN-rsFC was positively associated with cognitive control (Jilka et al., 2014) and creative thinking (Beaty et al., 2015), while it was reduced in patients with major depressive disorder (Sacchet et al., 2016, Yang et al., 2016).

In contrast, the switching between the SN and CEN was not directly (and globally) strengthened under GHB, as the inter-network connectivity between the SN and the CENs was not significantly increased. Actually, the switching between the SN and the CEN appeared indirectly (and locally) strengthened via the dorsal nexus hub, as this node showed increased connectivity to both the SN (via the anterior insula) and the CEN (via the MFG), albeit at the used statistical threshold, these effects were only significant for the right hemisphere (i.e. right anterior insula and right MFG). This however was also in line with previous ASL and rsFC results (Bosch et al., 2017a, Bosch et al., 2017b). Thus, GHB induced a complex pattern of functional connectivity increase encompassing all three core neurocognitive networks of the brain: the DMN, SN, and CEN.

Moreover, when both stimulation and sedation subjective ratings were jointly used as independent behavioral predictors for the local changes in the SN component scores in the

dorsal nexus region, a positive correlation was found for *sedation,* but not for *stimulation*, and similar trends were observed for the right anterior insula and the right middle frontal gyrus.
In the framework of the dorsal nexus biomarker of depression hypothesis, an increase of dorsal nexus -rsFC to dlPFC, which also belongs to the CEN, was interpreted as one of the antidepressive mechanisms of sleep deprivation (Bosch et al., 2013). Although GHB was shown to enhance mood in healthy subjects (Bosch et al., 2015), clinical evidence regarding GHB in depression is scarce (Bosch et al., 2012, Bosch and Seifritz, 2016, Mamelak, 2009). Therefore, no valid conclusion in respect of the relationship of GHB-induced dorsal nexus rsFC and depression can be drawn. However, in our study dorsal nexus connectivity effectively served as a biomarker for a subjective drug effect, in this case sedation, underlining its role as a central hub region and its usefulness in neuropsychopharmacological research.

Additional evidences for a complex neuronal equilibrium between stimulating and sedating effects of GHB derive from a recent study, where we assessed exact low resolution electromagnetic tomography of resting-state high-density electroencephalographic (EEG) recordings under influence of the drug in healthy humans (von Rotz et al., 2017). Our findings confirmed an earlier described “paradoxical EEG-behavioral dissociation” characterized by electrophysiological states that resemble loss of consciousness (mirrored in the emergence of low frequency oscillations) in awake and partially stimulated subjects. In these subjects, GHB led to the emergence of theta oscillations in the PCC (the same area we used as seed to assess DMN connectivity). Theta oscillations usually occur during sleep and would be expected to be paralleled by reduced rsFC within DMN (Samann et al., 2011). Contrary and intriguingly, theta oscillations occurred together with an increased intrinsic DMN-rsFC, which was positively correlated with GHB plasma values. Here, the seemingly paradoxical GHB effect of co-occurrence of electrophysiological sleep signs and alert wakefulness was explained by the

counterbalance of PCC-generated theta oscillations and strengthened connectivity within the DMN.

Taken together, subjective, fMRI, and EEG data emerging from studies on the effects of GHB show a coherent and unique neuropsychopharmacological signature. It consists of a subjective pattern of mixed stimulation and sedation, stable/increased DMN- and increased SN-, and dorsal nexus-, and indirectly also CEN-rsFC, as well as PCC-generated theta oscillation emergence. These alterations are most likely generated by a concert of primary GABAergic and secondary dopaminergic mechanisms, pharmacologically positioning GHB in between sedative drugs such as benzodiazepines and z-substances, and stimulants such as methylphenidate and modafinil. This “pluripotency” including mood and hedonia enhancement shown previously (Bosch et al., 2015, 2017a,b), makes GHB a unique and interesting research tool and experimental therapeutic in neuropsychiatric disorders, e.g., depression, but also a dangerous drug of abuse.

The present study bears a number of limitations: our sample size was moderate and limited to male subjects, as gender-dependent GHB effects on sexual arousal were tested in the fMRI part of the study (Bosch et al., 2017b). Moreover, we only used a single dose of GHB in this first attempt due to feasibility reasons. Further studies should therefore employ increased sample sizes, male and female subjects, and dose variations to confirm and extend the here reported results.

5. CONCLUSIONS

In summary, GHB exerts a mixed sedative-stimulant subjective effect, which is paralleled by increased intrinsic SN-rsFC to the dorsal nexus, and reciprocally increased dorsal nexus-rsFC to the SN (right anterior insula), as well as a CEN area, the right MFG. Moreover, rsFC between SN and DMN was also increased. Subjective sedation was mediated by increased SN-rsFC to

the dorsal nexus. Consequently, the subjective state induced by GHB is accompanied by a complex pattern of increased functional connectivity encompassing all three core neurocognitive networks of the brain (DMN, SN, CEN), while increased SN-dorsal nexus-rsFC was demonstrated to be a potential signature of the sedative component of the drug effect.

Acknowledgements

We would like to thank Sara Romer for her helpful assistance in data collection and in subject recruitment, as well as Dr. Marcus Herdener and Dr. Milan Scheidegger for their assistance in designing the fMRI set-up.

References

ABANADES, S., FARRE, M., SEGURA, M., PICHINI, S., BARRAL, D., PACIFICI, R., PELLEGRINI, M., FONSECA, F., LANGOHR, K. & DE LA TORRE, R. 2006. Gamma-hydroxybutyrate (GHB) in humans: pharmacodynamics and pharmacokinetics. *Ann N Y Acad Sci,* 1074**,** 559-76.

BEATY, R. E., BENEDEK, M., KAUFMAN, S. B. & SILVIA, P. J. 2015. Default and Executive Network Coupling Supports Creative Idea Production. *Sci Rep,* 5**,** 10964.

BENAVIDES, J., RUMIGNY, J. F., BOURGUIGNON, J. J., CASH, C., WERMUTH, C. G., MANDEL, P., VINCENDON, G. & MAITRE, M. 1982. High affinity binding sites for gamma-hydroxybutyric acid in rat brain. *Life Sci,* 30**,** 953-61.

BOSCH, O. G., QUEDNOW, B. B., SEIFRITZ, E. & WETTER, T. C. 2012. Reconsidering GHB: orphan drug or new model antidepressant? *J Psychopharmacol,* 26**,** 618-28.

BOSCH, O. G., RIHM, J. S., SCHEIDEGGER, M., LANDOLT, H. P., STAMPFLI, P., BRAKOWSKI, J., ESPOSITO, F., RASCH, B. & SEIFRITZ, E. 2013. Sleep deprivation increases dorsal nexus connectivity to the dorsolateral prefrontal cortex in humans. *Proc Natl Acad Sci U S A,* 110**,** 19597-602.

BOSCH, O. G., EISENEGGER, C., GERTSCH, J., VON ROTZ, R., DORNBIERER, D., GACHET, M. S., HEINRICHS, M., WETTER, T. C., SEIFRITZ, E. & QUEDNOW, B. B. 2015. Gamma-hydroxybutyrate enhances mood and prosocial behavior without affecting plasma oxytocin and testosterone. *Psychoneuroendocrinology,* 62**,** 1-10.

BOSCH, O. G. & SEIFRITZ, E. 2016. The behavioural profile of gamma-hydroxybutyrate, gamma-butyrolactone and 1,4-butanediol in humans. *Brain Res Bull*.

BOSCH, O. G., ESPOSITO, F., HAVRANEK, M. M., DORNBIERER, D., VON ROTZ, R., STAEMPFLI, P., QUEDNOW, B. B. & SEIFRITZ, E. 2017a. Gamma-Hydroxybutyrate Increases Resting-State Limbic Perfusion and Body and Emotion Awareness in Humans. *Neuropsychopharmacology*.

BOSCH, O. G., HAVRANEK, M. M., BAUMBERGER, A., PRELLER, K. H., VON ROTZ, R., HERDENER, M., KRAEHENMANN, R., STAEMPFLI, P., SCHEIDEGGER, M., KLUCKEN, T., SEIFRITZ, E. & QUEDNOW, B. B. 2017b. Neural underpinnings of prosexual effects induced by gamma-hydroxybutyrate in healthy male humans. *Eur Neuropsychopharmacol,* 27**,** 372-382.

BUCKNER, R. L., ANDREWS-HANNA, J. R. & SCHACTER, D. L. 2008. The brain's default network: anatomy, function, and relevance to disease. *Ann N Y Acad Sci,* 1124**,** 1-38.

CERA, N., TARTARO, A. & SENSI, S. L. 2014. Modafinil alters intrinsic functional connectivity of the right posterior insula: a pharmacological resting state fMRI study. *PLoS One,* 9**,** e107145.

CRAIG, A. D. 2009. How do you feel--now? The anterior insula and human awareness. *Nat Rev Neurosci,* 10**,** 59-70.

DE HAVAS, J. A., PARIMAL, S., SOON, C. S. & CHEE, M. W. 2012. Sleep deprivation reduces default mode network connectivity and anti-correlation during rest and task performance. *Neuroimage,* 59**,** 1745-51.

EKLUND, A., NICHOLS, T. E. & KNUTSSON, H. 2016. Cluster failure: Why fMRI inferences for spatial extent have inflated false-positive rates. *Proc Natl Acad Sci U S A,* 113**,** 7900-5.

ENGBERG, G. & NISSBRANDT, H. 1993. gamma-Hydroxybutyric acid (GHBA) induces pacemaker activity and inhibition of substantia nigra dopamine neurons by activating GABAB-receptors. *Naunyn Schmiedebergs Arch Pharmacol,* 348**,** 491-7.

ESPOSITO, F., SCARABINO, T., HYVARINEN, A., HIMBERG, J., FORMISANO, E., COMANI, S., TEDESCHI, G., GOEBEL, R., SEIFRITZ, E. & DI SALLE, F. 2005. Independent component analysis of fMRI group studies by self-organizing clustering. *Neuroimage,* 25**,** 193-205.

ESPOSITO, F., PIGNATARO, G., DI RENZO, G., SPINALI, A., PACCONE, A., TEDESCHI, G. & ANNUNZIATO, L. 2010. Alcohol increases spontaneous BOLD signal fluctuations in the visual network. *Neuroimage,* 53**,** 534-43.

ESPOSITO, F. & GOEBEL, R. 2011. Extracting functional networks with spatial independent component analysis: the role of dimensionality, reliability and aggregation scheme. *Curr Opin Neurol,* 24**,** 378-85.

ESPOSITO, F., OTTO, T., ZIJLSTRA, F. R. & GOEBEL, R. 2014. Spatially distributed effects of mental exhaustion on resting-state FMRI networks. *PLoS One,* 9**,** e94222.

ESPOSITO, R., CILLI, F., PIERAMICO, V., FERRETTI, A., MACCHIA, A., TOMMASI, M., SAGGINO, A., CIAVARDELLI, D., MANNA, A., NAVARRA, R., CIERI, F., STUPPIA, L., TARTARO, A. & SENSI, S. L. 2013. Acute effects of modafinil on brain resting state networks in young healthy subjects. *PLoS One,* 8**,** e69224.

FARR, O. M., ZHANG, S., HU, S., MATUSKEY, D., ABDELGHANY, O., MALISON, R. T. & LI, C. S. 2014. The effects of methylphenidate on resting-state striatal, thalamic and global functional connectivity in healthy adults. *Int J Neuropsychopharmacol,* 17**,** 1177-91.

FIRST, M. B., SPITZER, R. L., GIBBON, M. & WILLIAMS, J. B. W. 2002. *Structured Clinical Interview for DSM-IV-TR Axis I Disorders, Research Version, Non-patient Edition,* New York.

FORMAN, S. D., COHEN, J. D., FITZGERALD, M., EDDY, W. F., MINTUN, M. A. & NOLL, D. C. 1995. Improved assessment of significant activation in functional magnetic resonance imaging (fMRI): use of a cluster-size threshold. *Magn Reson Med,* 33**,** 636-47.

FOX, M. D. & RAICHLE, M. E. 2007. Spontaneous fluctuations in brain activity observed with functional magnetic resonance imaging. *Nat Rev Neurosci,* 8**,** 700-11.

FRISTON, K. J., WILLIAMS, S., HOWARD, R., FRACKOWIAK, R. S. & TURNER, R. 1996. Movement-related effects in fMRI time-series. *Magn Reson Med,* 35**,** 346-55.

GEERLIGS, L., TSVETANOV, K. A., CAM, C. & HENSON, R. N. 2017. Challenges in measuring individual differences in functional connectivity using fMRI: The case of healthy aging. *Hum Brain Mapp,* 38**,** 4125-4156.

GOGOLLA, N., TAKESIAN, A. E., FENG, G., FAGIOLINI, M. & HENSCH, T. K. 2014. Sensory integration in mouse insular cortex reflects GABA circuit maturation. *Neuron,* 83**,** 894-905.

GREICIUS, M. D., SRIVASTAVA, G., REISS, A. L. & MENON, V. 2004. Default-mode network activity distinguishes Alzheimer's disease from healthy aging: evidence from functional MRI. *Proc Natl Acad Sci U S A,* 101**,** 4637-42.

GREICIUS, M. D., FLORES, B. H., MENON, V., GLOVER, G. H., SOLVASON, H. B., KENNA, H., REISS, A. L. & SCHATZBERG, A. F. 2007. Resting-state functional connectivity in major depression: abnormally increased contributions from subgenual cingulate cortex and thalamus. *Biol Psychiatry,* 62**,** 429-37.

GREICIUS, M. D., KIVINIEMI, V., TERVONEN, O., VAINIONPAA, V., ALAHUHTA, S., REISS, A. L. & MENON, V. 2008. Persistent default-mode network connectivity during light sedation. *Hum Brain Mapp,* 29**,** 839-47.

HOROVITZ, S. G., BRAUN, A. R., CARR, W. S., PICCHIONI, D., BALKIN, T. J., FUKUNAGA, M. & DUYN, J. H. 2009. Decoupling of the brain's default mode network during deep sleep. *Proc Natl Acad Sci U S A,* 106**,** 11376-81.

HYVARINEN, A. 1999. Fast and robust fixed-point algorithms for independent component analysis. *IEEE Trans Neural Netw,* 10**,** 626-34.

JILKA, S. R., SCOTT, G., HAM, T., PICKERING, A., BONNELLE, V., BRAGA, R. M., LEECH, R. & SHARP, D. J. 2014. Damage to the Salience Network and interactions with the Default Mode Network. *J Neurosci,* 34**,** 10798-807.

KAPITANY-FOVENY, M., MERVO, B., CORAZZA, O., KOKONYEI, G., FARKAS, J., URBAN, R., ZACHER, G. & DEMETROVICS, Z. 2015. Enhancing sexual desire and experience: an investigation of the sexual correlates of gamma-hydroxybutyrate (GHB) use. *Hum Psychopharmacol,* 30**,** 276-84.

KHALILI-MAHANI, N., ZOETHOUT, R. M., BECKMANN, C. F., BAERENDS, E., DE KAM, M. L., SOETER, R. P., DAHAN, A., VAN BUCHEM, M. A., VAN GERVEN, J. M. & ROMBOUTS, S. A. 2012. Effects of

morphine and alcohol on functional brain connectivity during "resting state": a placebo-controlled crossover study in healthy young men. *Hum Brain Mapp,* 33**,** 1003-18.
KHALSA, S., MAYHEW, S. D., CHECHLACZ, M., BAGARY, M. & BAGSHAW, A. P. 2014. The structural and functional connectivity of the posterior cingulate cortex: comparison between deterministic and probabilistic tractography for the investigation of structure-function relationships. *Neuroimage,* 102 Pt 1**,** 118-27.
KIVINIEMI, V. J., HAANPAA, H., KANTOLA, J. H., JAUHIAINEN, J., VAINIONPAA, V., ALAHUHTA, S. & TERVONEN, O. 2005. Midazolam sedation increases fluctuation and synchrony of the resting brain BOLD signal. *Magn Reson Imaging,* 23**,** 531-7.
KLINE, R. L., ZHANG, S., FARR, O. M., HU, S., ZABORSZKY, L., SAMANEZ-LARKIN, G. R. & LI, C. S. 2016. The Effects of Methylphenidate on Resting-State Functional Connectivity of the Basal Nucleus of Meynert, Locus Coeruleus, and Ventral Tegmental Area in Healthy Adults. *Front Hum Neurosci,* 10**,** 149.
KOECHLIN, E. & SUMMERFIELD, C. 2007. An information theoretical approach to prefrontal executive function. *Trends Cogn Sci,* 11**,** 229-35.
KONOVA, A. B., MOELLER, S. J., TOMASI, D. & GOLDSTEIN, R. Z. 2015. Effects of chronic and acute stimulants on brain functional connectivity hubs. *Brain Res,* 1628**,** 147-56.
LARSON-PRIOR, L. J., ZEMPEL, J. M., NOLAN, T. S., PRIOR, F. W., SNYDER, A. Z. & RAICHLE, M. E. 2009. Cortical network functional connectivity in the descent to sleep. *Proc Natl Acad Sci U S A,* 106**,** 4489-94.
LEHRL, S. 2005. *Mehrfachwahl-Wortschatz-Intelligenztest: MWT-B,* Balingen.
LI, S. J., BISWAL, B., LI, Z., RISINGER, R., RAINEY, C., CHO, J. K., SALMERON, B. J. & STEIN, E. A. 2000. Cocaine administration decreases functional connectivity in human primary visual and motor cortex as detected by functional MRI. *Magn Reson Med,* 43**,** 45-51.
LIANG, P., ZHANG, H., XU, Y., JIA, W., ZANG, Y. & LI, K. 2015. Disruption of cortical integration during midazolam-induced light sedation. *Hum Brain Mapp,* 36**,** 4247-61.
LICATA, S. C., NICKERSON, L. D., LOWEN, S. B., TRKSAK, G. H., MACLEAN, R. R. & LUKAS, S. E. 2013. The hypnotic zolpidem increases the synchrony of BOLD signal fluctuations in widespread brain networks during a resting paradigm. *Neuroimage,* 70**,** 211-22.
LIECHTI, M. E., QUEDNOW, B. B., LIAKONI, E., DORNBIERER, D., VON ROTZ, R., GACHET, M. S., GERTSCH, J., SEIFRITZ, E. & BOSCH, O. G. 2016. Pharmacokinetics and pharmacodynamics of gamma-hydroxybutyrate in healthy subjects. *Br J Clin Pharmacol,* 81**,** 980-8.
MAMELAK, M. 2009. Narcolepsy and depression and the neurobiology of gammahydroxybutyrate. *Prog Neurobiol,* 89**,** 193-219.
MARKETT, S., REUTER, M., MONTAG, C., VOIGT, G., LACHMANN, B., RUDORF, S., ELGER, C. E. & WEBER, B. 2014. Assessing the function of the fronto-parietal attention network: insights from resting-state fMRI and the attentional network test. *Hum Brain Mapp,* 35**,** 1700-9.
MCCABE, C., MISHOR, Z., FILIPPINI, N., COWEN, P. J., TAYLOR, M. J. & HARMER, C. J. 2011. SSRI administration reduces resting state functional connectivity in dorso-medial prefrontal cortex. *Mol Psychiatry,* 16**,** 592-4.
MENON, V. & UDDIN, L. Q. 2010. Saliency, switching, attention and control: a network model of insula function. *Brain Struct Funct,* 214**,** 655-67.
MENON, V. 2011. Large-scale brain networks and psychopathology: a unifying triple network model. *Trends Cogn Sci,* 15**,** 483-506.
MENON, V. 2015. *Salience Network,* London, Oxford, Boston, New York, San Diego, Elsevier Academic Press.
MUELLER, S., COSTA, A., KEESER, D., POGARELL, O., BERMAN, A., COATES, U., REISER, M. F., RIEDEL, M., MOLLER, H. J., ETTINGER, U. & MEINDL, T. 2014. The effects of methylphenidate on whole brain intrinsic functional connectivity. *Hum Brain Mapp,* 35**,** 5379-88.

NIENDAM, T. A., LAIRD, A. R., RAY, K. L., DEAN, Y. M., GLAHN, D. C. & CARTER, C. S. 2012. Meta-analytic evidence for a superordinate cognitive control network subserving diverse executive functions. *Cogn Affect Behav Neurosci,* 12**,** 241-68.

POWER, J. D., BARNES, K. A., SNYDER, A. Z., SCHLAGGAR, B. L. & PETERSEN, S. E. 2012. Spurious but systematic correlations in functional connectivity MRI networks arise from subject motion. *Neuroimage,* 59**,** 2142-54.

POWER, J. D., SCHLAGGAR, B. L. & PETERSEN, S. E. 2015. Recent progress and outstanding issues in motion correction in resting state fMRI. *Neuroimage,* 105**,** 536-51.

QUEDNOW, B. B., KUHN, K. U., HOENIG, K., MAIER, W. & WAGNER, M. 2004. Prepulse inhibition and habituation of acoustic startle response in male MDMA ('ecstasy') users, cannabis users, and healthy controls. *Neuropsychopharmacology,* 29**,** 982-90.

RAICHLE, M. E., MACLEOD, A. M., SNYDER, A. Z., POWERS, W. J., GUSNARD, D. A. & SHULMAN, G. L. 2001. A default mode of brain function. *Proc Natl Acad Sci U S A,* 98**,** 676-82.

RAICHLE, M. E. 2015. The brain's default mode network. *Annu Rev Neurosci,* 38**,** 433-47.

RAMAEKERS, J. G., EVERS, E. A., THEUNISSEN, E. L., KUYPERS, K. P., GOULAS, A. & STIERS, P. 2013. Methylphenidate reduces functional connectivity of nucleus accumbens in brain reward circuit. *Psychopharmacology (Berl),* 229**,** 219-26.

RISSANEN, J. 1978. Modeling by shortest data description. *Automatica* 14**,** 465-471.

SACCHET, M. D., HO, T. C., CONNOLLY, C. G., TYMOFIYEVA, O., LEWINN, K. Z., HAN, L. K., BLOM, E. H., TAPERT, S. F., MAX, J. E., FRANK, G. K., PAULUS, M. P., SIMMONS, A. N., GOTLIB, I. H. & YANG, T. T. 2016. Large-Scale Hypoconnectivity Between Resting-State Functional Networks in Unmedicated Adolescent Major Depressive Disorder. *Neuropsychopharmacology,* 41**,** 2951-2960.

SALMERON, B. J. & STEIN, E. A. 2002. Pharmacological applications of magnetic resonance imaging. *Psychopharmacol Bull,* 36**,** 102-29.

SAMANN, P. G., TULLY, C., SPOORMAKER, V. I., WETTER, T. C., HOLSBOER, F., WEHRLE, R. & CZISCH, M. 2010. Increased sleep pressure reduces resting state functional connectivity. *MAGMA,* 23**,** 375-89.

SAMANN, P. G., WEHRLE, R., HOEHN, D., SPOORMAKER, V. I., PETERS, H., TULLY, C., HOLSBOER, F. & CZISCH, M. 2011. Development of the brain's default mode network from wakefulness to slow wave sleep. *Cereb Cortex,* 21**,** 2082-93.

SATTERTHWAITE, T. D., ELLIOTT, M. A., GERRATY, R. T., RUPAREL, K., LOUGHEAD, J., CALKINS, M. E., EICKHOFF, S. B., HAKONARSON, H., GUR, R. C., GUR, R. E. & WOLF, D. H. 2013. An improved framework for confound regression and filtering for control of motion artifact in the preprocessing of resting-state functional connectivity data. *Neuroimage,* 64**,** 240-56.

SCHEIDEGGER, M., WALTER, M., LEHMANN, M., METZGER, C., GRIMM, S., BOEKER, H., BOESIGER, P., HENNING, A. & SEIFRITZ, E. 2012. Ketamine decreases resting state functional network connectivity in healthy subjects: implications for antidepressant drug action. *PLoS One,* 7**,** e44799.

SCHRANTEE, A., FERGUSON, B., STOFFERS, D., BOOIJ, J., ROMBOUTS, S. & RENEMAN, L. 2016. Effects of dexamphetamine-induced dopamine release on resting-state network connectivity in recreational amphetamine users and healthy controls. *Brain Imaging Behav,* 10**,** 548-58.

SEELEY, W. W., MENON, V., SCHATZBERG, A. F., KELLER, J., GLOVER, G. H., KENNA, H., REISS, A. L. & GREICIUS, M. D. 2007. Dissociable intrinsic connectivity networks for salience processing and executive control. *J Neurosci,* 27**,** 2349-56.

SHELINE, Y. I., PRICE, J. L., YAN, Z. & MINTUN, M. A. 2010. Resting-state functional MRI in depression unmasks increased connectivity between networks via the dorsal nexus. *Proc Natl Acad Sci U S A,* 107**,** 11020-5.

SHIRER, W. R., JIANG, H., PRICE, C. M., NG, B. & GREICIUS, M. D. 2015. Optimization of rs-fMRI Pre-processing for Enhanced Signal-Noise Separation, Test-Retest Reliability, and Group Discrimination. *Neuroimage,* 117**,** 67-79.

SMITH, S. M., FOX, P. T., MILLER, K. L., GLAHN, D. C., FOX, P. M., MACKAY, C. E., FILIPPINI, N., WATKINS, K. E., TORO, R., LAIRD, A. R. & BECKMANN, C. F. 2009. Correspondence of the brain's functional architecture during activation and rest. *Proc Natl Acad Sci U S A,* 106**,** 13040-5.

SPRENG, R. N., SEPULCRE, J., TURNER, G. R., STEVENS, W. D. & SCHACTER, D. L. 2013. Intrinsic architecture underlying the relations among the default, dorsal attention, and frontoparietal control networks of the human brain. *J Cogn Neurosci,* 25**,** 74-86.

SRIPADA, C. S., KESSLER, D., WELSH, R., ANGSTADT, M., LIBERZON, I., PHAN, K. L. & SCOTT, C. 2013. Distributed effects of methylphenidate on the network structure of the resting brain: a connectomic pattern classification analysis. *Neuroimage,* 81**,** 213-21.

SUMNALL, H. R., WOOLFALL, K., EDWARDS, S., COLE, J. C. & BEYNON, C. M. 2008. Use, function, and subjective experiences of gamma-hydroxybutyrate (GHB). *Drug Alcohol Depend,* 92**,** 286-90.

TELTZROW, R. & BOSCH, O. G. 2012. Ecstatic anaesthesia: Ketamine and GHB between medical use and self-experimentation. *Applied Cardiopulmonary Pathophysiology,* 16**,** 309-321.

THAI, D., DYER, J. E., JACOB, P. & HALLER, C. A. 2007. Clinical pharmacology of 1,4-butanediol and gamma-hydroxybutyrate after oral 1,4-butanediol administration to healthy volunteers. *Clin Pharmacol Ther,* 81**,** 178-84.

TORO, R., FOX, P. T. & PAUS, T. 2008. Functional coactivation map of the human brain. *Cereb Cortex,* 18**,** 2553-9.

TSVETANOV, K. A., HENSON, R. N., TYLER, L. K., RAZI, A., GEERLIGS, L., HAM, T. E., ROWE, J. B., CAMBRIDGE CENTRE FOR, A. & NEUROSCIENCE 2016. Extrinsic and Intrinsic Brain Network Connectivity Maintains Cognition across the Lifespan Despite Accelerated Decay of Regional Brain Activation. *J Neurosci,* 36**,** 3115-26.

VAN DEN HEUVEL, M. P., MANDL, R. C., KAHN, R. S. & HULSHOFF POL, H. E. 2009. Functionally linked resting-state networks reflect the underlying structural connectivity architecture of the human brain. *Hum Brain Mapp,* 30**,** 3127-41.

VARIKUTI, D. P., HOFFSTAEDTER, F., GENON, S., SCHWENDER, H., REID, A. T. & EICKHOFF, S. B. 2017. Resting-state test-retest reliability of a priori defined canonical networks over different preprocessing steps. *Brain Struct Funct,* 222**,** 1447-1468.

VON ROTZ, R., KOMETER, M., DORNBIERER, D., GERTSCH, J., SALOME GACHET, M., VOLLENWEIDER, F. X., SEIFRITZ, E., BOSCH, O. G. & QUEDNOW, B. B. 2017. Neuronal oscillations and synchronicity associated with gamma-hydroxybutyrate during resting-state in healthy male volunteers. *Psychopharmacology (Berl),* 234**,** 1957-1968.

WANG, C., ONG, J. L., PATANAIK, A., ZHOU, J. & CHEE, M. W. 2016. Spontaneous eyelid closures link vigilance fluctuation with fMRI dynamic connectivity states. *Proc Natl Acad Sci U S A,* 113**,** 9653-8.

YAN, C. G., CRADDOCK, R. C., HE, Y. & MILHAM, M. P. 2013. Addressing head motion dependencies for small-world topologies in functional connectomics. *Front Hum Neurosci,* 7**,** 910.

YANG, R., GAO, C., WU, X., YANG, J., LI, S. & CHENG, H. 2016. Decreased functional connectivity to posterior cingulate cortex in major depressive disorder. *Psychiatry Res,* 255**,** 15-23.

ZUO, X. N., DI MARTINO, A., KELLY, C., SHEHZAD, Z. E., GEE, D. G., KLEIN, D. F., CASTELLANOS, F. X., BISWAL, B. B. & MILHAM, M. P. 2010. The oscillating brain: complex and reliable. *Neuroimage,* 49**,** 1432-45.

Figure Legends

Fig. 1: Effects on visual analogue scale (VAS) scores of GHB vs. placebo for *general drug effect*, *sedation*, and *stimulation*. ***p<.001, **p<.01, *p<.05 (Bonferroni-corrected).

Fig. 2: Main effects of the group components corresponding to the networks of interest as obtained from the group-level from independent component analysis of all baseline scans.

Fig. 3: Contrast of GHB vs. placebo effects on salience network from independent component analysis including time-course of effects, all FWE-corrected and including time-course of resting-state functional connectivity changes, ***p<.005.

Fig. 4: Overlap of region of salience network connectivity increase under GHB (turquoise) and a priori defined dorsal nexus (brown).

Fig. 5: Dorsal nexus resting-state functional connectivity changes GHB vs. placebo: A) Dorsal nexus seed location, B) whole-brain dorsal nexus connectivity map, C) right anterior insula, D) right middle frontal gyrus, all FWE-corrected and including time-course of resting-state functional connectivity changes, ***p<.001, **p<.005. MFG: middle frontal gyrus.

Fig. 6: A) Right anterior insula (peak of dorsal nexus connectivity) vs. salience network map, B) Right middle frontal gyrus (peak of dorsal nexus connectivity) vs. right central executive network map.

Fig. 7: Overlap of GHB-induced increase of dorsal nexus connectivity to right anterior insula (orange) and regional cerebral blood flow increase to right anterior insula after GHB (from Bosch et al. 2017a).

Figure 1

Click here to download 9. Figure: Figure 1 VAS ratings.pptx

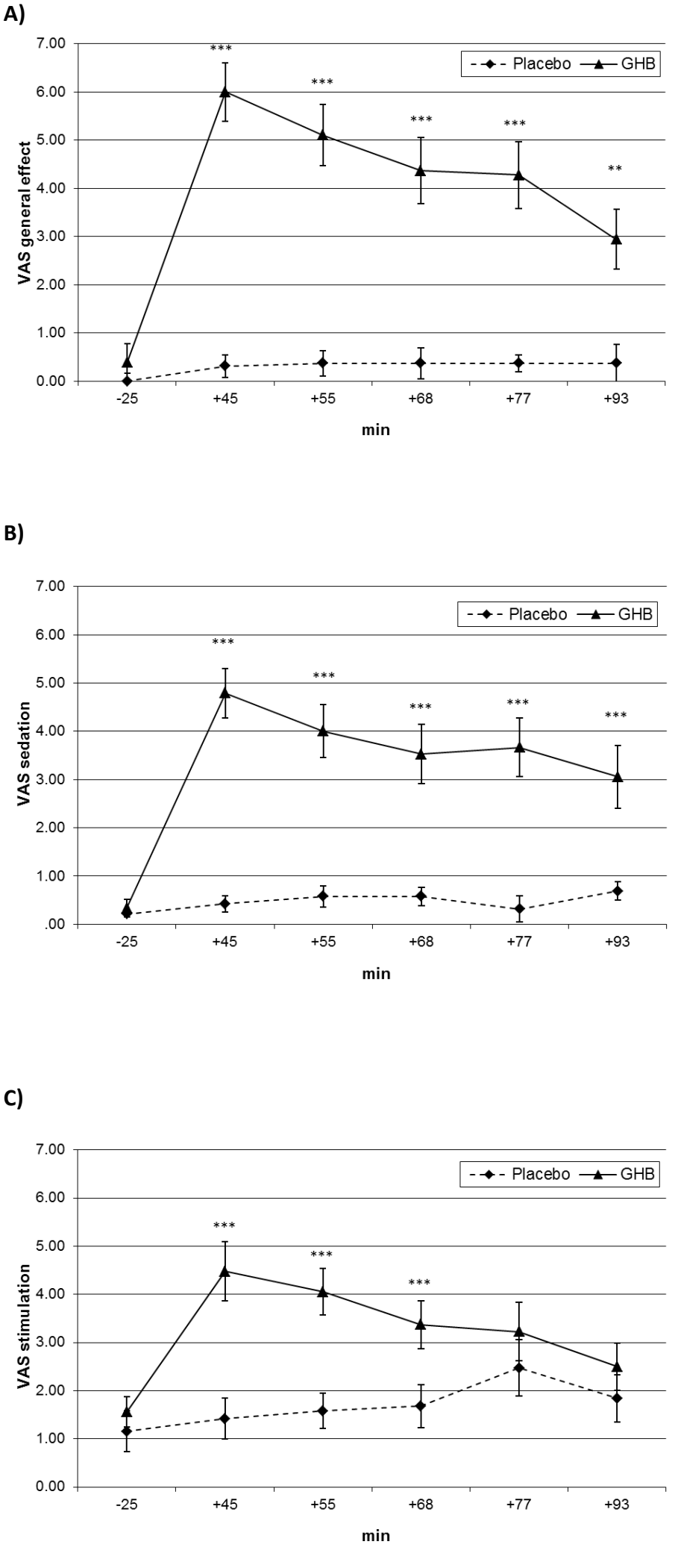

Click here to download 9. Figure: Figure 2 ICA all networks baseline.pptx

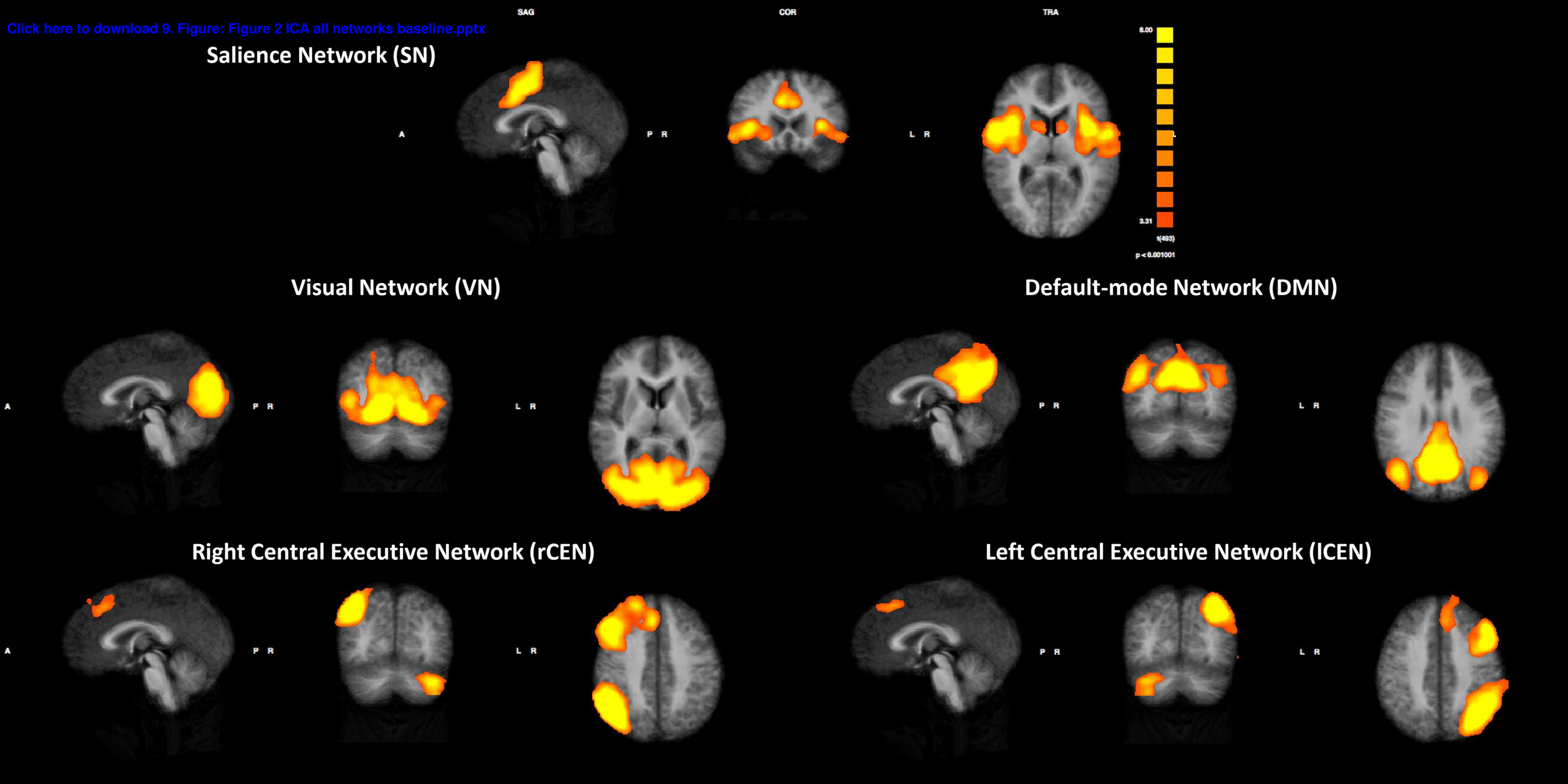

Salience Network (ICA)

[GHB (34 min) – GHB (baseline)] vs. [Placebo (34 min) – Placebo (baseline)]

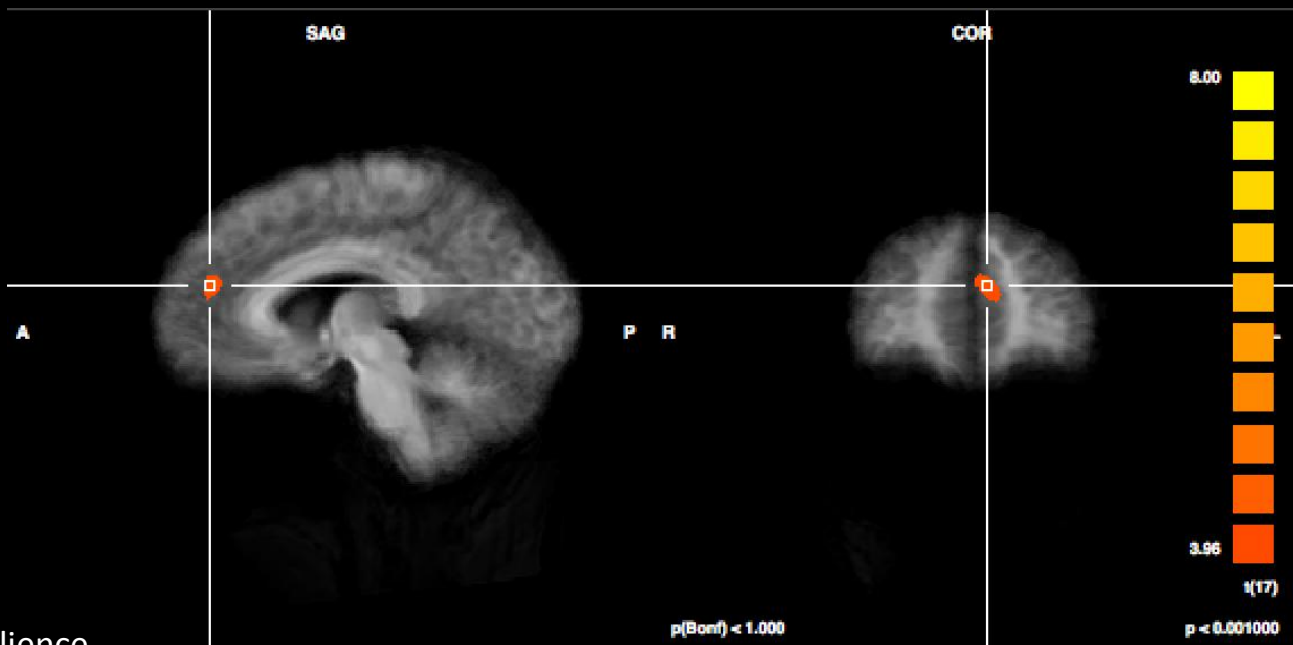

Network: Salience
Region: dorsomedial prefrontal cortex
(-6,46,19) /Dorsal Nexus

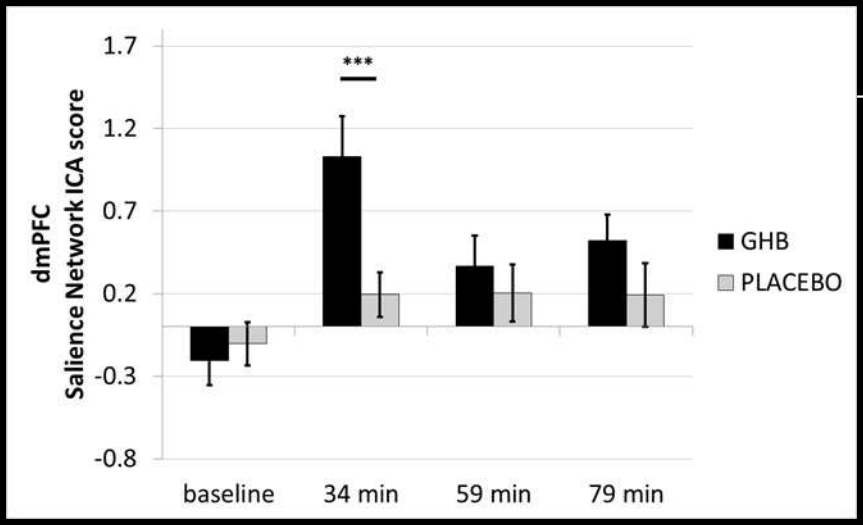

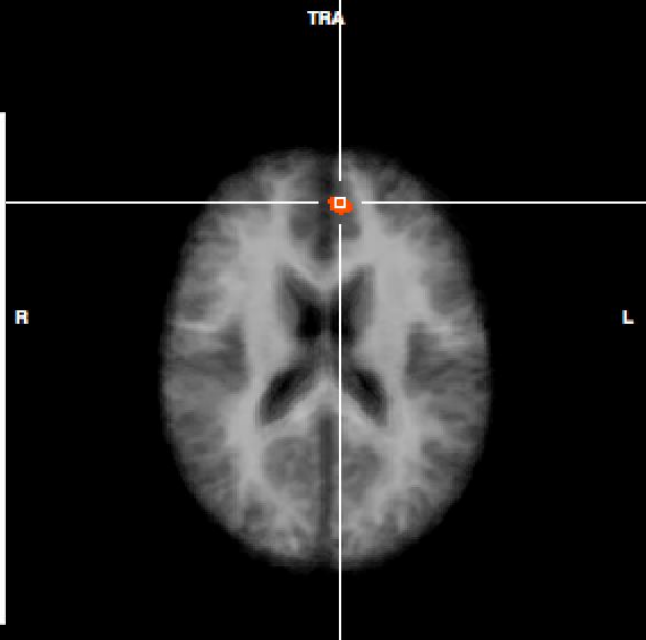

Click here to download 9. Figure: Figure 4 SN - DN OVERLAP.pptx

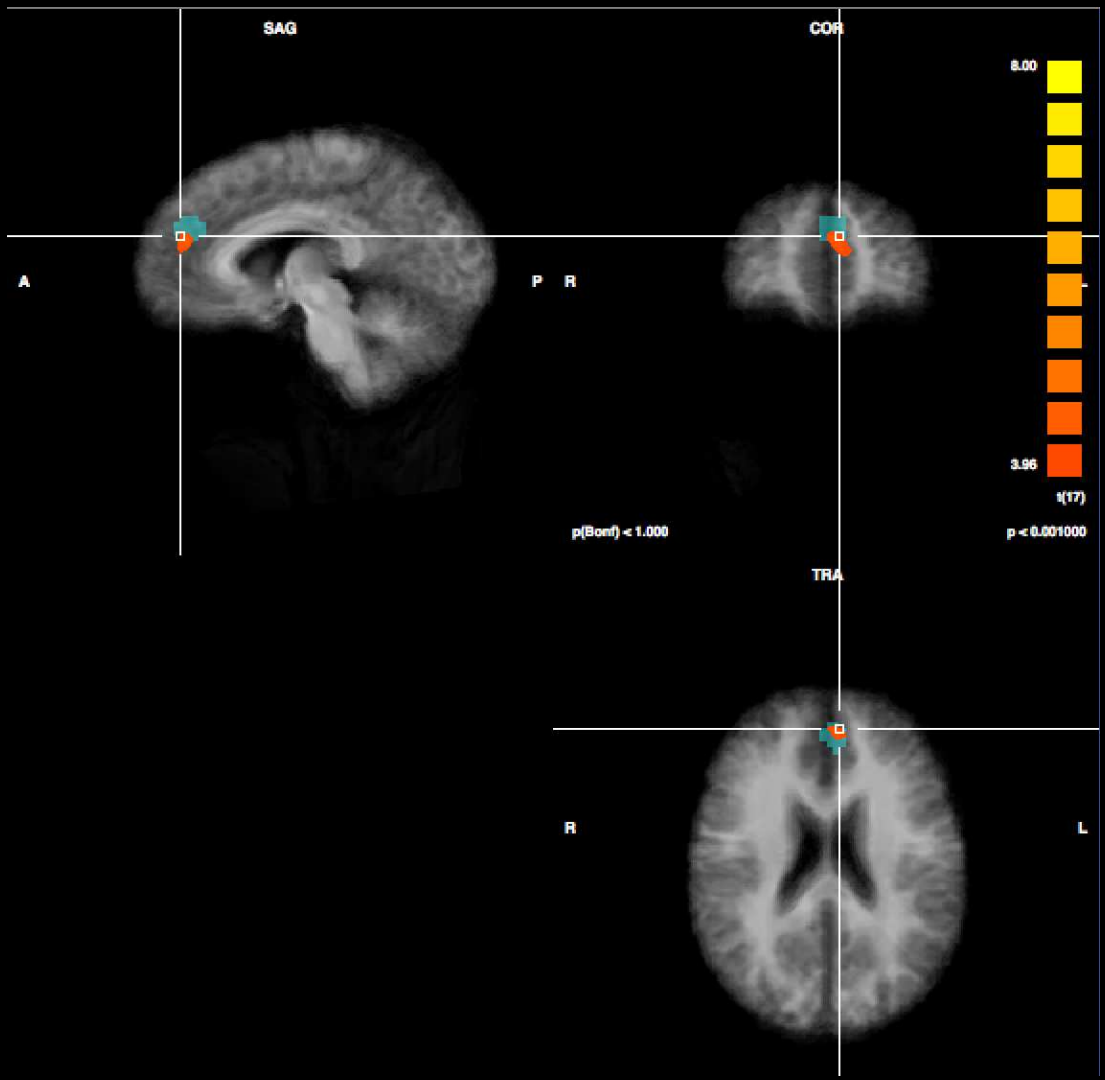

Click here to download 9. Figure: Figure 5 DN FC.pptx

A) Dorsal nexus seed location

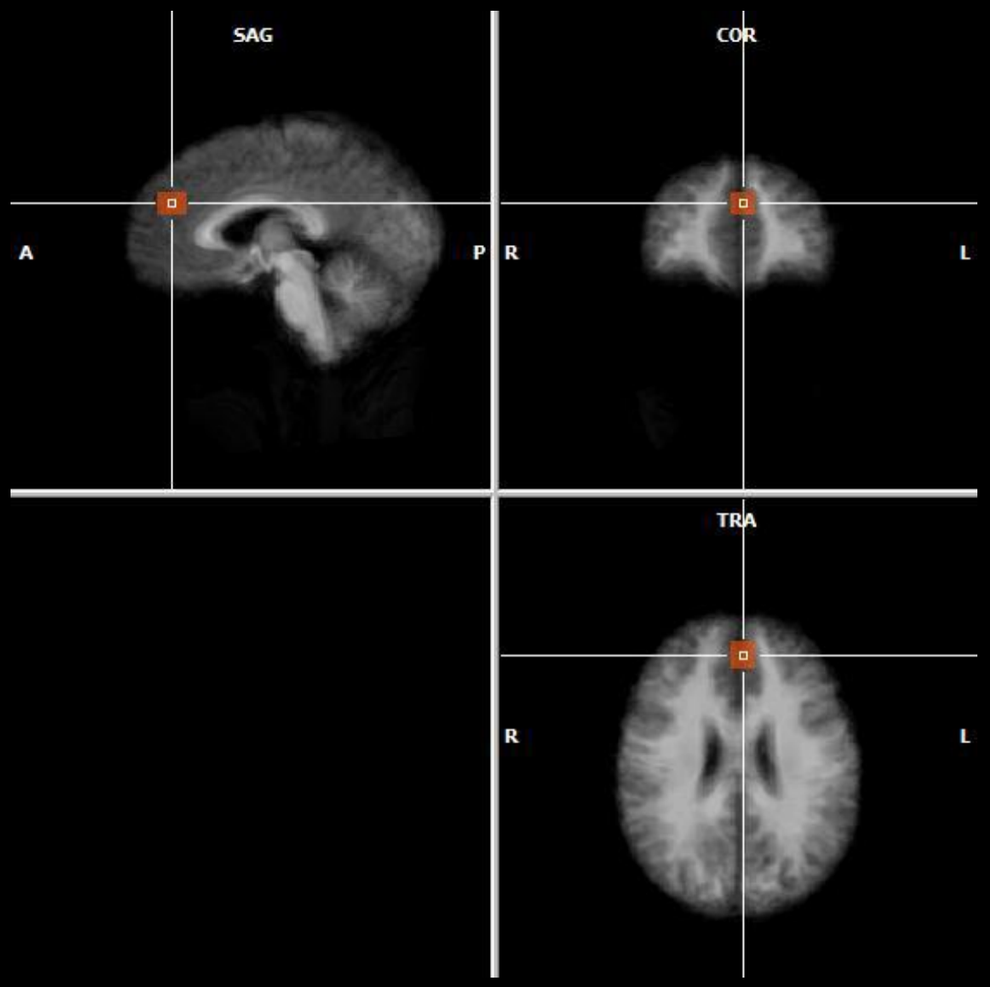

B) Whole-brain dorsal nexus connectivity map

[GHB (34 min) – GHB (baseline)] vs. [Placebo (34 min) – Placebo (baseline)]

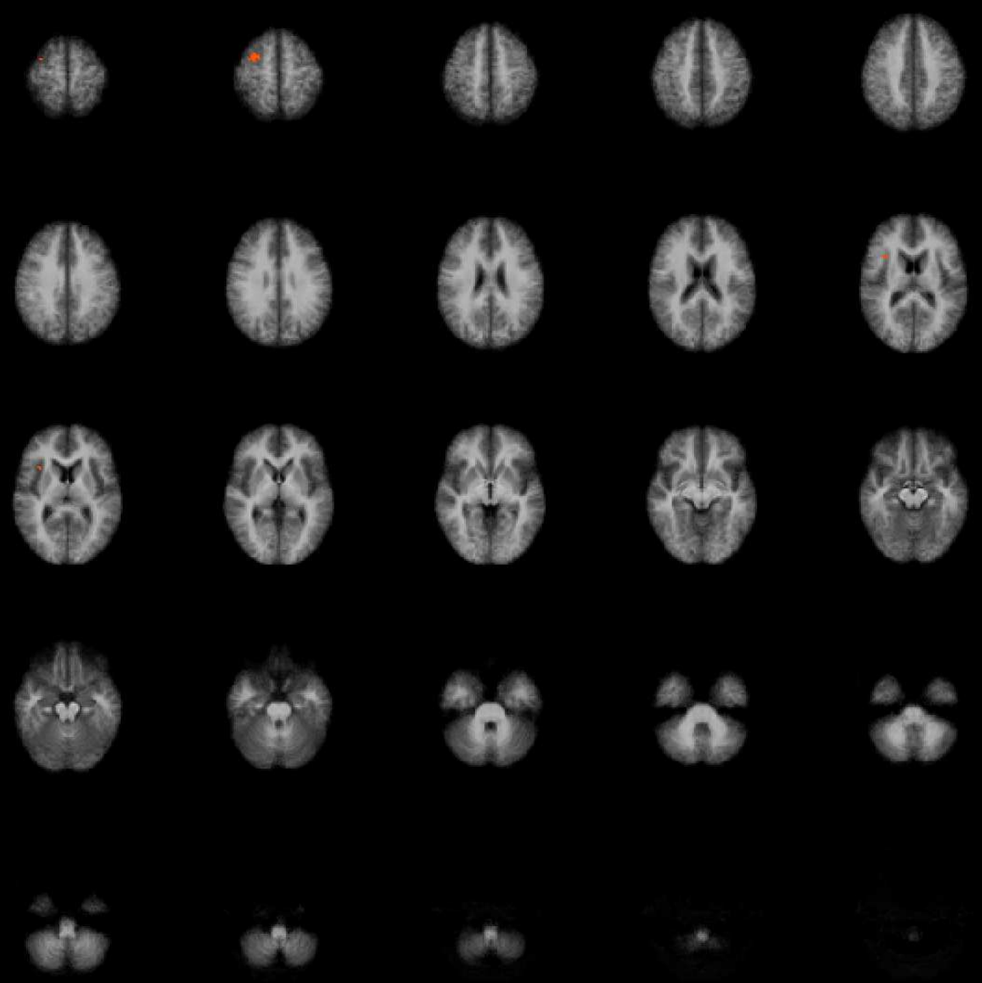

C) Right anterior insula

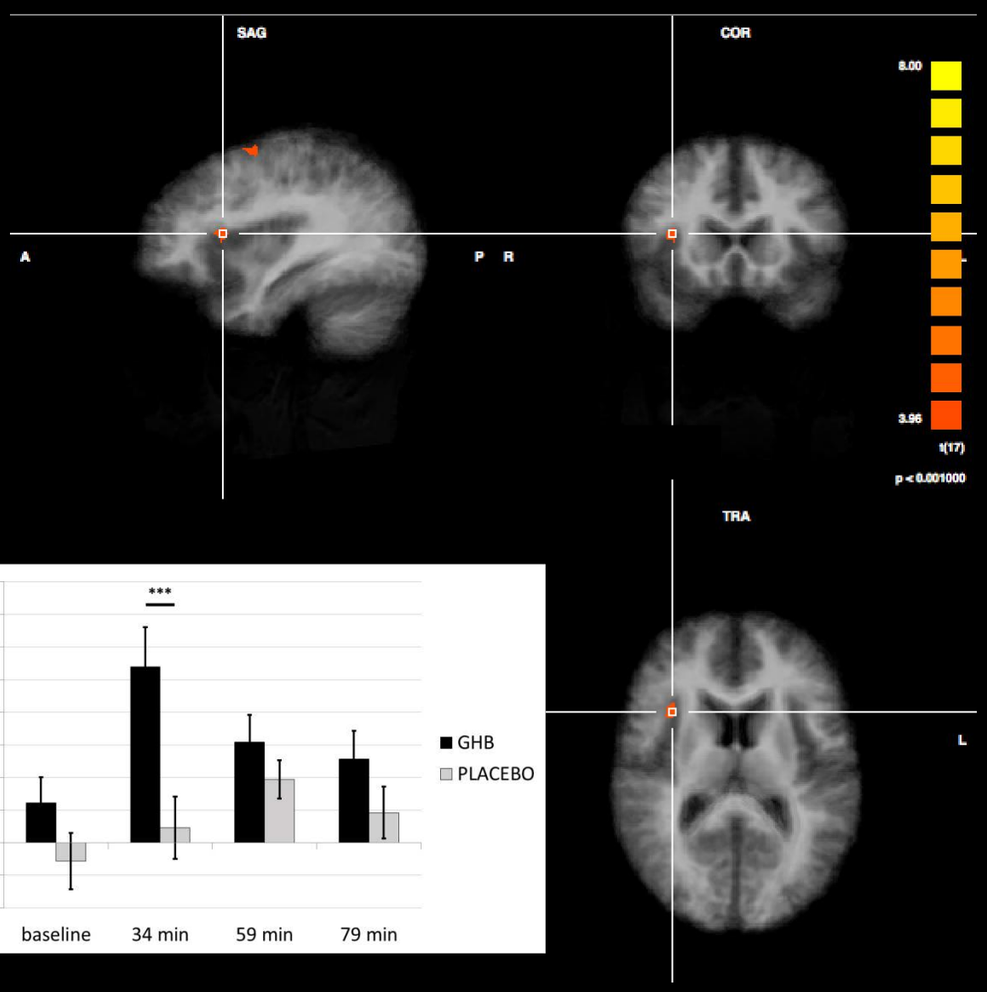

D) Right middle frontal gyrus

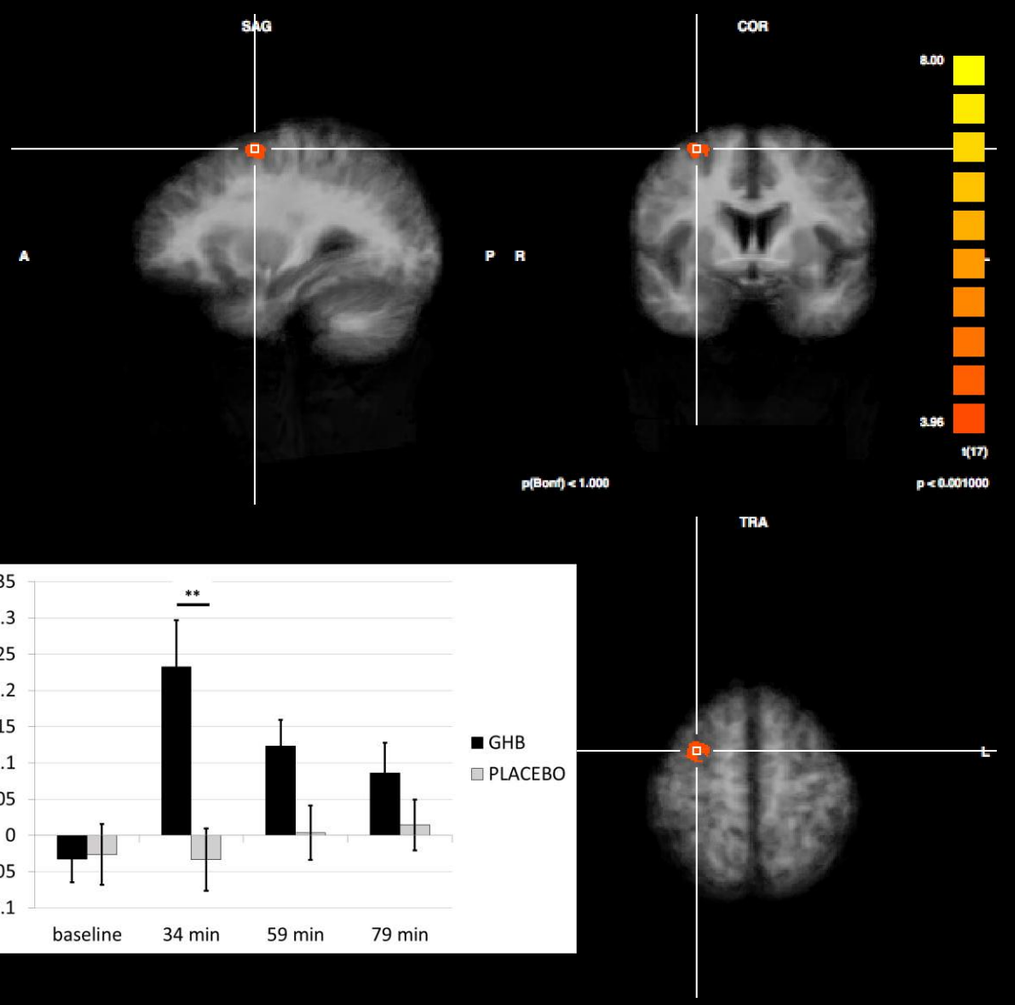

Click here to download 9. Figure: Figure 6 DN-FC vs. ICA SN-CEN OVERLAP.pptx

A) Right anterior insula (peak of dorsal nexus connectivity) vs. salience network map

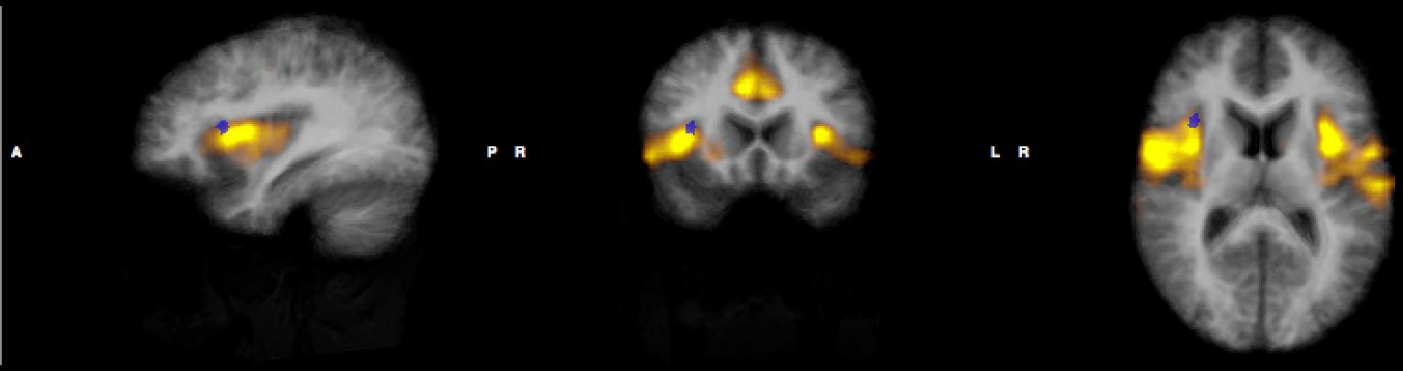

B) Right middle frontal gyrus (peak of dorsal nexus connectivity) vs. right central executive network map

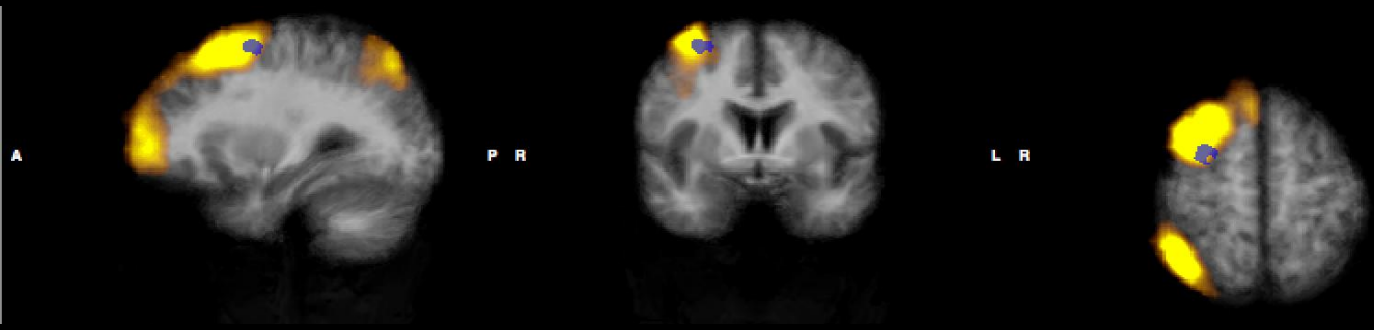

Click here to download 9. Figure: Figure 7 RST ASL Insula OVERLAP.pptx

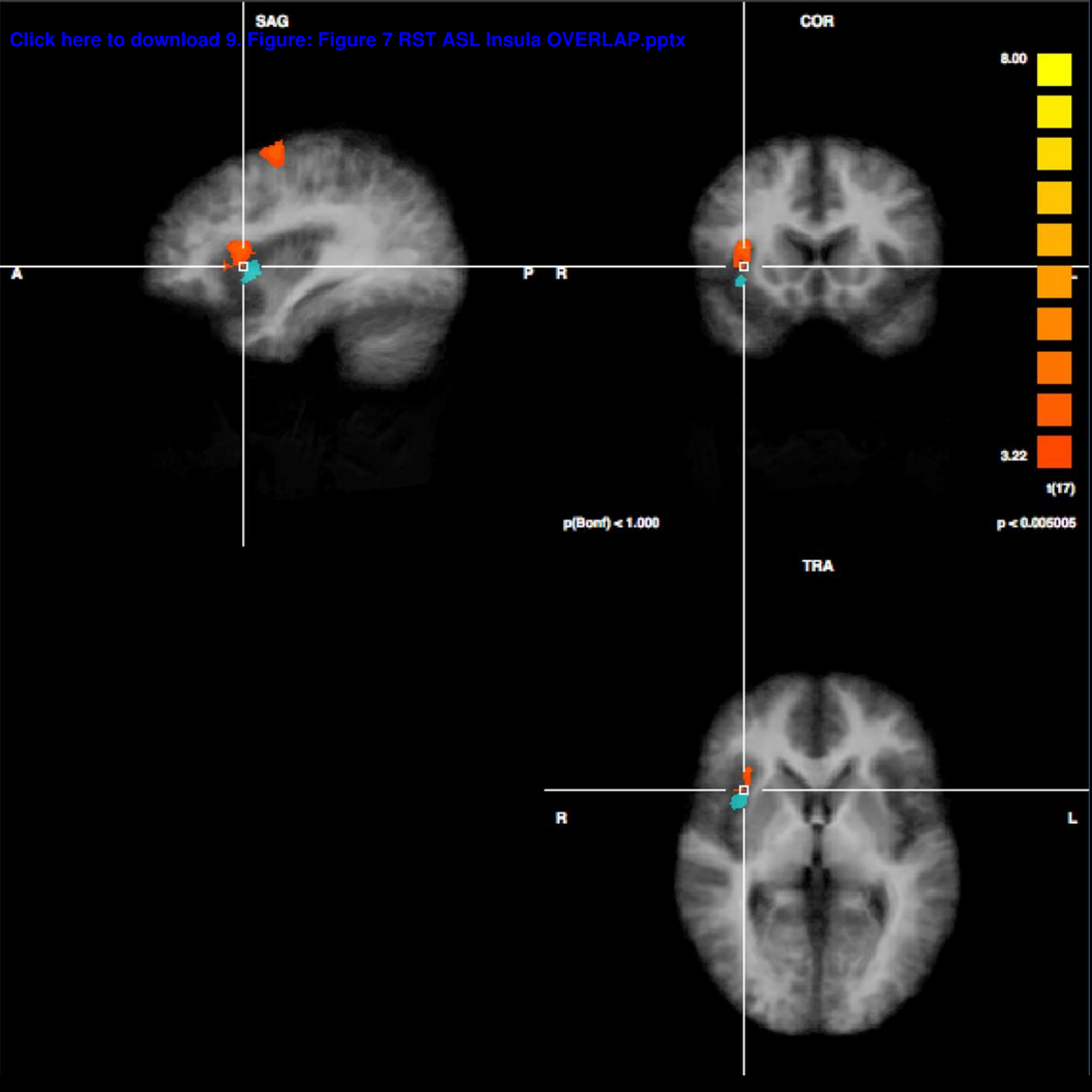

Gamma-hydroxybutyrate increases brain resting-state functional connectivity of the salience network and dorsal nexus in humans

Supplementary Material

Oliver G. Bosch[a,b,*], MD, Fabrizio Esposito[c], PhD, Dario Dornbierer[a,b], Msc, Michael M. Havranek[a], MD, PhD, Robin von Rotz[a,b], BSc, Michael Kometer[a], PhD, Philipp Staempfli[d], PhD , Boris B. Quednow[b,e], PhD, Erich Seifritz[a,e], MD

[a]*Department of Psychiatry, Psychotherapy and Psychosomatics, Psychiatric Hospital of the University of Zurich, Switzerland*
[b]*Experimental and Clinical Pharmacopsychology, Department of Psychiatry, Psychotherapy and Psychosomatics, Psychiatric Hospital of the University of Zurich, Switzerland*
[c]*Department of Medicine, Surgery and Dentistry "Scuola Medica Salernitana", University of Salerno, 84081 Baronissi, Italy*
[d]*MR-Center of the Department of Psychiatry, Psychotherapy and Psychosomatics and the Department of Child and Adolescent Psychiatry, Psychiatric Hospital of the University of Zurich, 8032 Zurich, Switzerland*
[e]*Neuroscience Center Zurich, University and ETH Zurich, Switzerland*

Supplementary Figure 1

Time point	Task
t – 28 min	VAS 1
t – 25 min	scan preparation
t – 20 min	baseline-RST scan
t – 14 min	baseline-ASL scan
t – 09 min	baseline anatomy scan
t – 06 min	scan termination
t_0	**GHB / placebo application**
t + 05 min	pause
t + 30 min	scan preparation
t + 34 min	RST scan 1
t + 40 min	ASL scan 1
t + 45 min	VAS 2
t + 48 min	task scan 1
t + 55 min	VAS 3
t + 59 min	RST scan 2
t + 65 min	ASL scan 2
t + 68 min	VAS 4
t + 70 min	task scan 2
t + 77 min	VAS 5
t + 79 min	RST scan 3
t + 85 min	ASL scan 3
t + 90 min	post-task anatomy
t + 93 min	VAS 6
t + 95 min	scan termination
t + 109 min	**session ending**

Session procedure. VAS: visual analog scale, RST: resting-state, ASL: arterial spin labeling, GHB: gamma-hydroxybutyrate.

Supplementary Figure 2

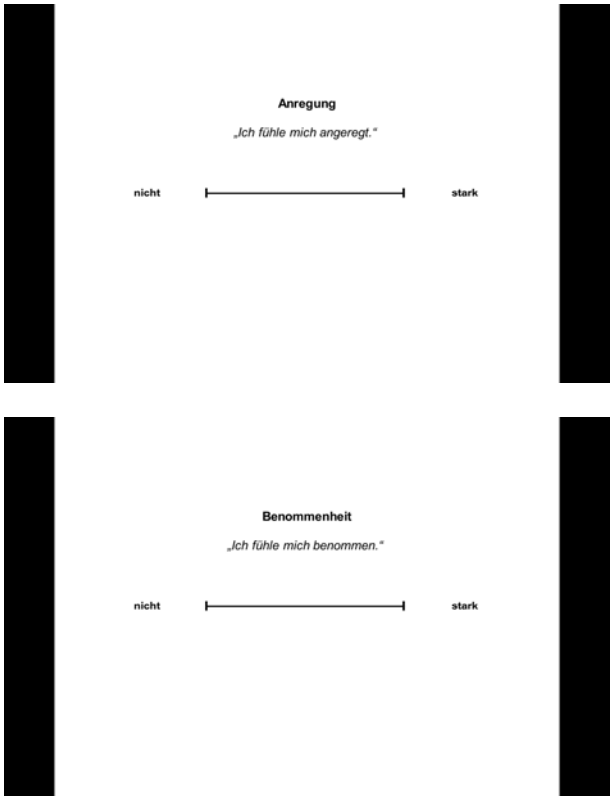

Visual analog scale, items “general drug effect”, “stimulation, and “sedation” (German version).

Supplementary Figure 3

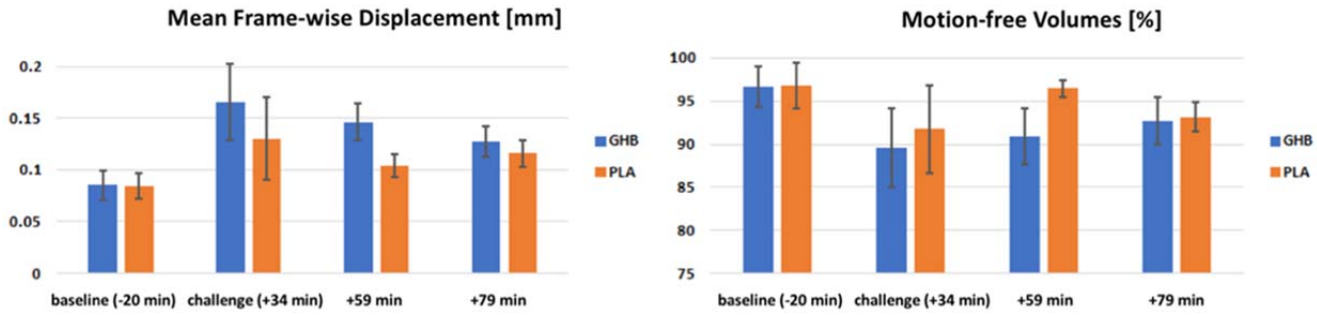

Mean frame-wise displacement [mm] (left) and percentage of motion-free volumes (right) across scans and conditions (GHB vs PLACEBO).

Supplementary Figure 4

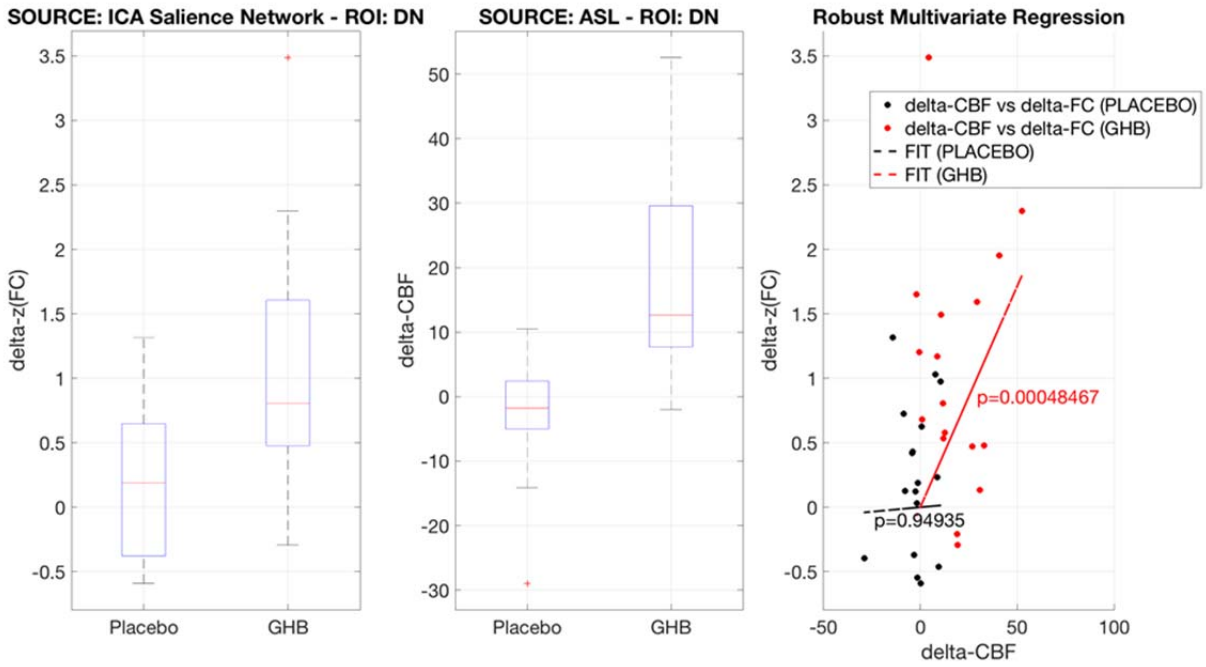

Box (left, center) and scatter (right) plots of the local increases in salience network component scores (challenge vs. baseline) and in cerebral blood flow [ml/100g/min] (challenge vs. baseline) from corresponding arterial spin labeling scans (see Bosch et al., 2017a for details) in dmPFC/dorsal nexus. Trend lines and statistical significances of the correlations (robust multivariate regression) are shown on the scatter plot.

Supplementary Figure 5

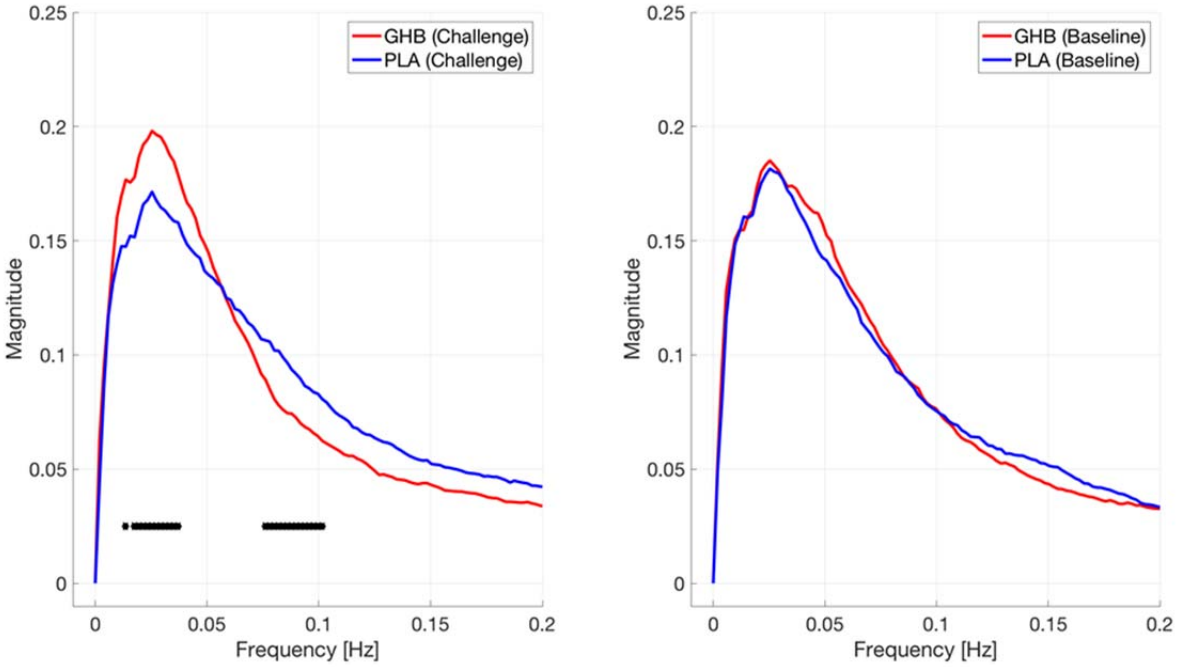

Average of all smoothed magnitude FFT spectra of the salience network component time-courses from all challenge and baseline scans (grouped by condition and time point) (GHB vs. placebo). Black asterisks are placed at frequency bins where the difference between conditions is statistically significant (paired t-test, $p<=0.05$).

Supplementary Figure 6

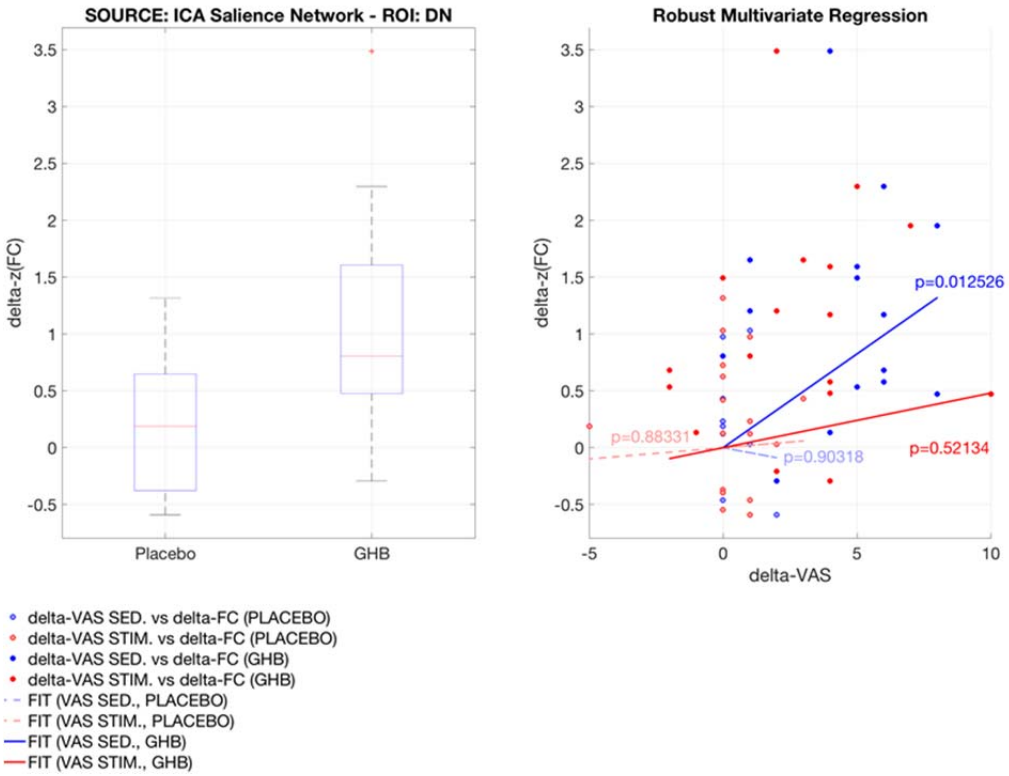

Left: Box plot of the changes (challenge vs. baseline) in the regional salience network component scores (Δ_FC) in dorsal nexus (DN). Right: Stimulation and sedation subjective ratings as two independent predictors for the regional salience network component scores in dorsal nexus (robust multivariate regression analysis): statistically significant ($p<.05$) correlation between Δ_FC and Δ_VAS for sedation at +34 min ($p=0.013$), but not for stimulation ($p>0.05$), under GHB, but not under placebo ($p>0.05$). Trend lines and statistical significances of the correlations (robust multivariate regression) are shown on the scatter plot of Δ_FC and Δ_VAS measures.

Supplementary Figure 7

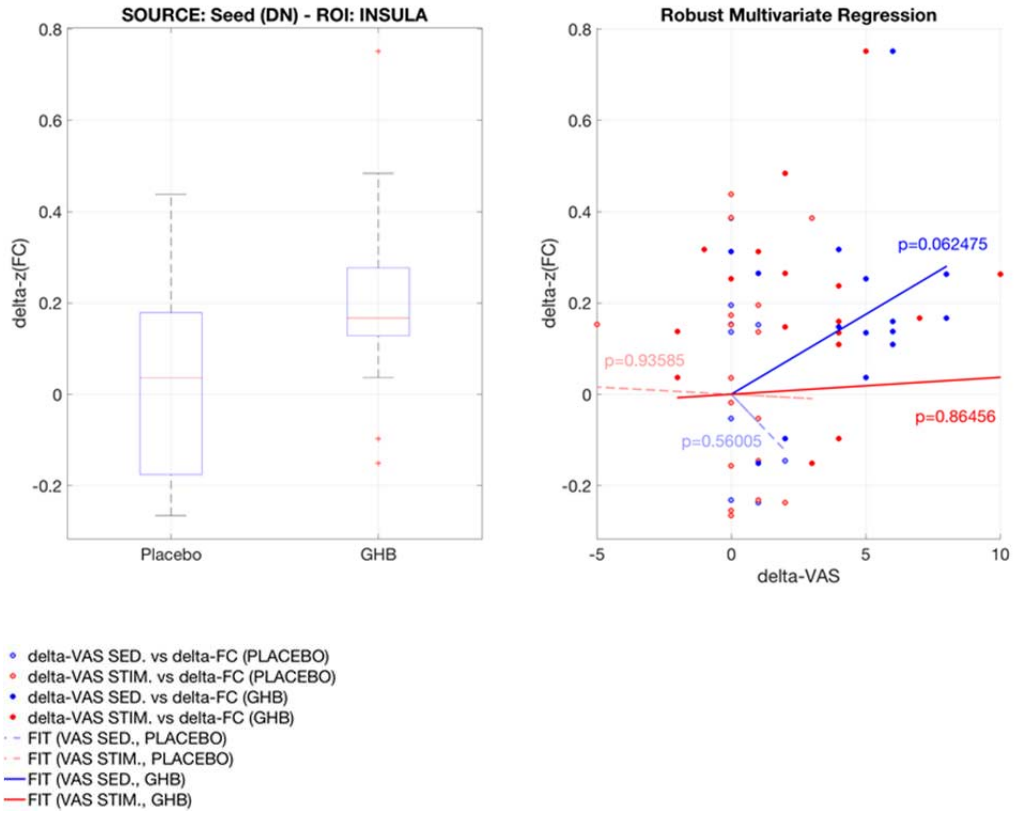

Left: Box plot of the changes (challenge vs. baseline) in the regional functional connectivity scores (Δ_FC) from the dorsal nexus (DN) seed in the right anterior insula. Right: Stimulation and sedation subjective ratings as two independent predictors for the regional functional connectivity scores in the right anterior insula (robust multivariate regression analysis): trend correlations between Δ_FC and Δ_VAS are more evident for sedation at +34 min (p=0.062), than for stimulation (p>0.1), under GHB, but not under placebo (p>0.1). Trend lines and statistical significances of these correlations (robust multivariate regression) are shown on the scatter plot of Δ_FC and Δ_VAS measures.

Supplementary Figure 8

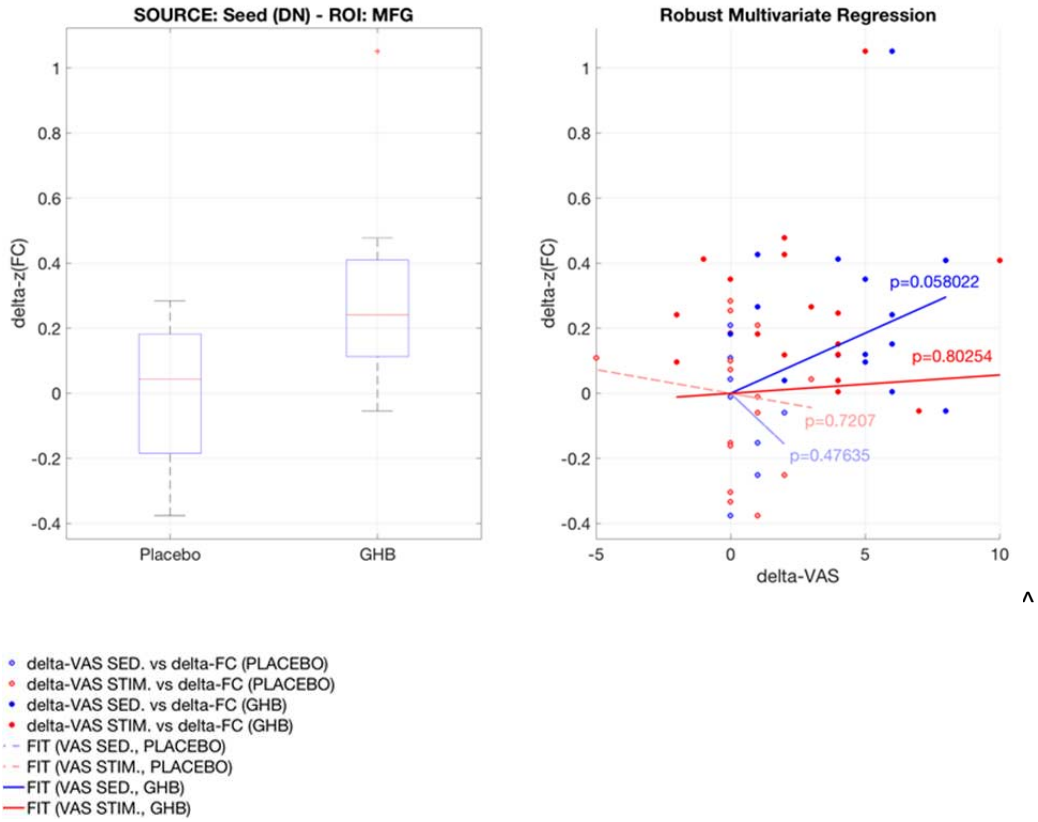

Left: Box plot of the changes (challenge vs. baseline) in the regional functional connectivity scores (Δ_FC) from the dorsal nexus (DN) seed in the right middle frontal gyrus (MFG). Right: Stimulation and sedation subjective ratings as two independent predictors for the regional functional connectivity scores in the right MFG (robust multivariate regression analysis): trend correlations between Δ_FC and Δ_VAS are more evident for sedation at +34 min (p=0.058), than for stimulation (p>0.1), under GHB, but not under placebo (p>0.1). Trend lines and statistical significances of these correlations (robust multivariate regression) are shown on the scatter plot of Δ_FC and Δ_VAS measures.

Supplementary Figure 9

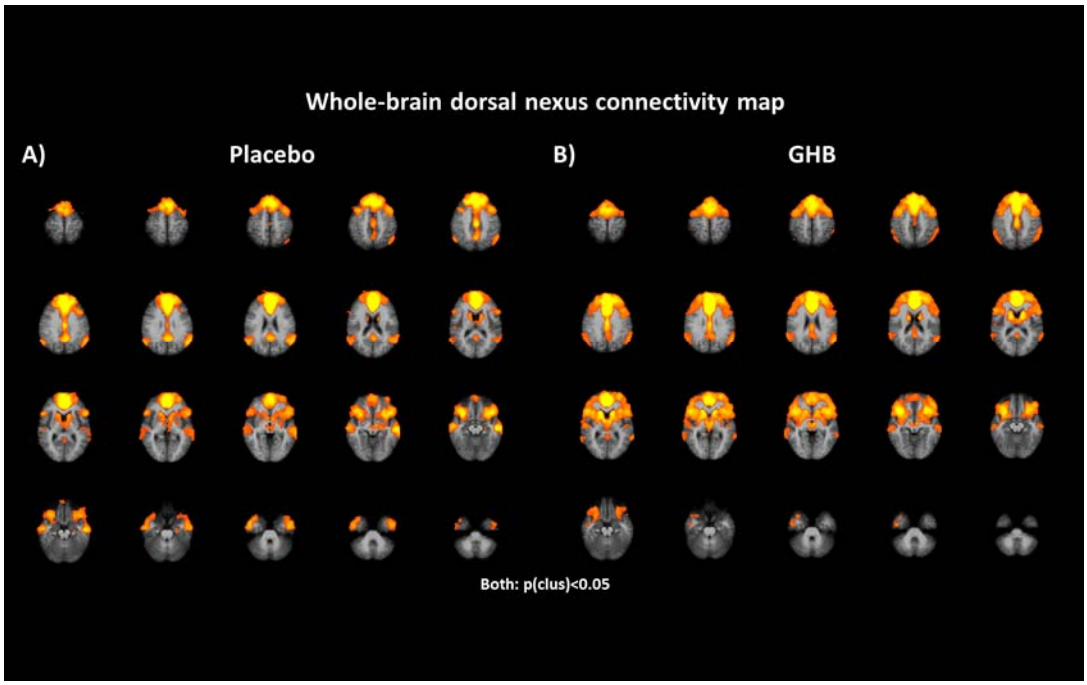

Whole-brain dorsal nexus resting state functional connectivity map, A) placebo, B) GHB at 34 min. p<.05 (cluster corrected).